YGS Open File 2025-8

Analysis of geoscience data for geothermal exploration in the Whitehorse area, Yukon

J.B. Witter

Yukon

Published under the authority of the Department of Energy, Mines and Resources, Government of Yukon https://yukon.ca/en/department-energy-mines-resources.

Publié avec l'autorisation du Ministères de l'Énergie, des Mines et des Ressources du gouvernement du Yukon, https://yukon.ca/en/department-energy-mines-resources.

This, and other Yukon Geological Survey publications, may be obtained from:

Yukon Geological Survey
102-300 Main Street
Box 2703 (K-102)
Whitehorse, Yukon, Canada Y1A 2C6

email geology@yukon.ca

Visit the Yukon Geological Survey website at https://yukon.ca/en/science-and-natural-resources/geology.

In referring to this publication, please use the following citation:

Witter, J.B., 2025. Analysis of geoscience data for geothermal exploration in the Whitehorse area, Yukon. Government of Yukon, Yukon Geological Survey, Open File 2025-8, 53 p. plus appendices.

Front cover: Photo of the City of Whitehorse facing north. Photo credit: Fritz Mueller.

Yukon

YGS Open File
2025-8

Analysis of geoscience data for geothermal exploration in the Whitehorse area, Yukon

Jeffrey B. Witter
Innovate Geothermal Ltd.

Innovate Geothermal

Table of Contents

Abstract

In collaboration with the Yukon Geological Survey, and other project partners, Innovate Geothermal Ltd. performed an analysis of geoscience data in a 13 by 15 km area in the northern part of the City of Whitehorse to better understand the potential for geothermal energy resources that, if present, could be used for heating purposes. The primary goal of this project is to analyze and interpret a variety of pre-existing and newly-acquired geological and geophysical datasets to evaluate where geothermal reservoirs may be present within the study area. A secondary goal is to propose favourable drilling locations, if warranted, for exploratory boreholes to collect information on subsurface temperature and permeability. The geoscience work accomplished here includes both 2D map interpretation as well as construction of a 3D geologic model that was guided by geophysical inversion modelling of gravity and magnetic survey data. At a regional scale, multiple lines of evidence suggest that subsurface temperatures are above the crustal average. More importantly, three warm springs located in the northwestern part of the city (Porter Creek and Crestview subdivisions) produce 12.0–18.5°C water and have water chemistry that suggest much higher temperature (minimum 54–87°C) geothermal fluids at depth. Existing data suggests that the warm springs are likely heated by natural radioactive decay in rocks of the Haeckel Hill pluton that underlies the Mount Sumanik area, northwest of Whitehorse. Additional geothermal aquifers with more modest temperature (~9°C or higher) are associated with the Miles Canyon basalt rock unit in the southeastern part of the study area. Both areas merit further geoscience studies to better characterize the subsurface. In the vicinity of the warm springs, three, 1 km deep, exploratory boreholes are proposed to obtain direct information on subsurface stratigraphy, temperature, and permeability. The central and southwestern portions of the study area are underlain by granitic rocks of the Whitehorse batholith and are considered geothermally unfavourable because mineral exploration boreholes that have been drilled into the batholith reveal subsurface temperatures that are below average for continental crust.

Plain language summary

This study presents the results of an analysis of geoscience data that helps define the geothermal potential for the northern part of the City of Whitehorse. Results indicate good potential for direct-use heating where warm springs are present in Porter Creek and Crestview subdivisions. Warm water could also be present below Riverdale subdivision. The area west of the Alaska Highway and south of the Fish Lake Road are considered less favourable to host a geothermal resource.

Introduction

Whitehorse is the largest city in northern Canada and the capital of the Yukon with a population of approximately 35 000 residents (Fig. 1). The city obtains electrical energy from a variety of hydroelectric (70%), wind (<1%), and fossil fuel (30%) facilities (Government of Yukon, 2018). These facilities are connected on an isolated electric transmission grid that serves multiple communities in southern and central Yukon. In contrast, space heating in Yukon buildings is primarily provided by fossil fuels (75%), wood (17%) and electricity (8%) (Government of Yukon, 2018).

Energy derived from subterranean geothermal reservoirs in the Whitehorse area could be beneficial in two different ways: 1) hot water from higher temperature (e.g. ~60°C) geothermal reservoirs could be used to directly heat buildings; and 2) warm water from lower temperature geothermal reservoirs (e.g. ~10–20°C) could be fed into heat pumps to reduce the amount of externally-derived fossil or electrical energy needed for space heating. In addition, warm geothermal fluids can be used for a variety of other applications such as greenhouses, aquaculture, snow-melting and de-icing, heating water for public swimming pools and food drying.

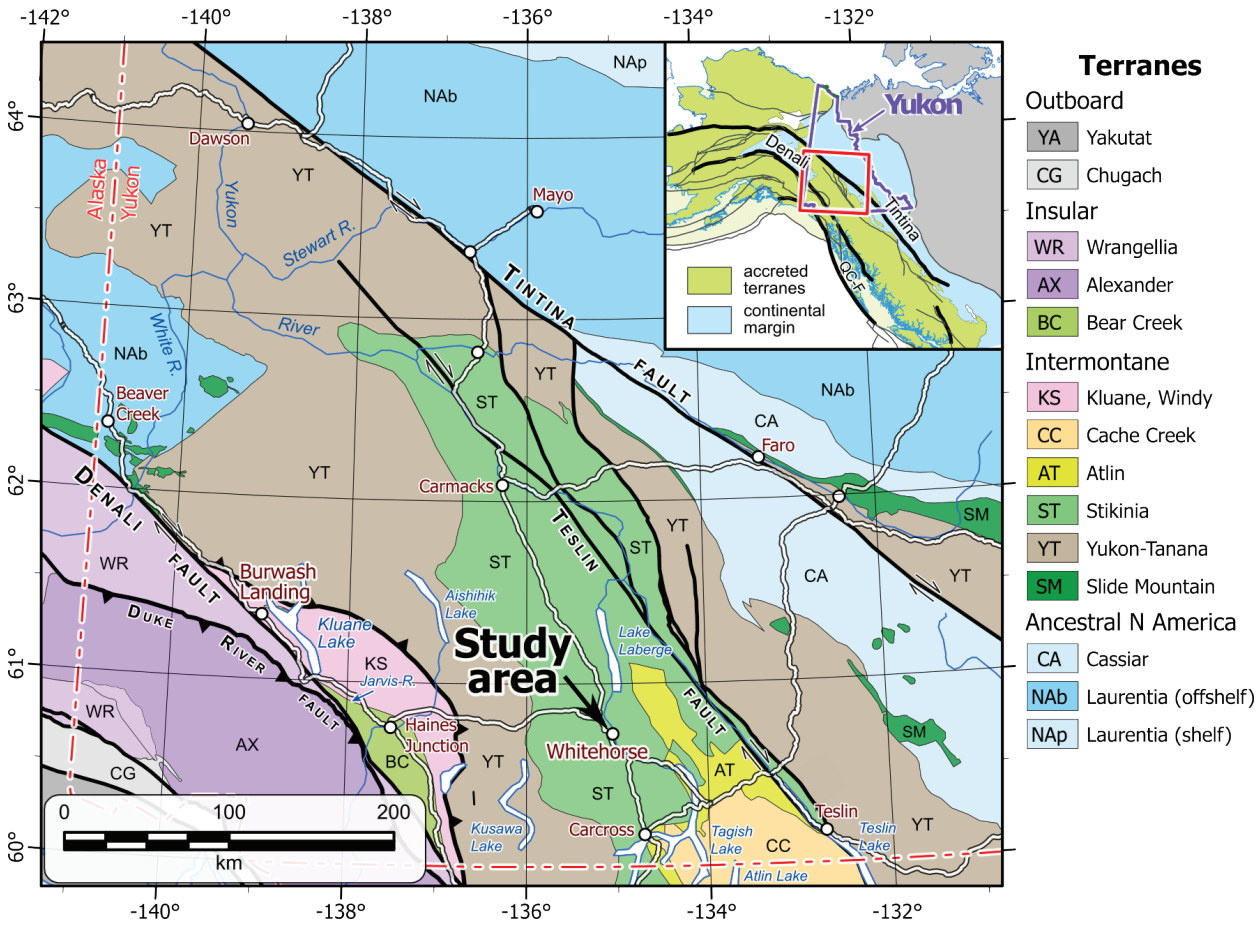

Figure 1. *Geologic map of southern Yukon illustrating the location of the study area described in this report. Geologic terrane basemap from Yukon Geological Survey (2023a). Black lines depict major faults. Red dashed lines show provincial/territorial borders. Inset indicates location of the Yukon in the Cordilleran mountain belt.*

Successful development of a natural geothermal resource requires two features in the subsurface: elevated temperature and rock permeability. Existing geoscience data suggest that there are above average subsurface temperatures in the Whitehorse region. For example, Curie point depth (CPD) mapping suggests an average, crustal-scale temperature gradient of ~42 to 48°C/km for Whitehorse, which is higher than the average thermal gradient of continental crust (~25°C/km). In addition, warm springs located in the northwestern part of the city (Porter Creek and Crestview subdivisions) have surface discharge temperatures of 12.0 to 18.5°C (Yukon Geological Survey, 2024). For comparison, typical shallow groundwater temperatures in the Whitehorse area are 2 to 5°C (EBA Engineering Consultants Ltd., 2009).

Interestingly, these warm springs occur at three locations, over a distance of ~6 km, at the interface between two specific rock types: the Hancock limestone and the Mandanna sandstone. This suggests that the geologic contact between these rock units may play a role in allowing the warm fluids to make their way to the surface.

Permeability in the subsurface (i.e., fractures and/or pore space in rock) allows geothermal fluids to flow through the rock into the wellbore of a geothermal production well. Three types of potentially permeable material that could host geothermal aquifers beneath Whitehorse are: 1) porous sediments (e.g., sand and gravel); 2) faulted and fractured bedrock; and 3) porous sedimentary rock (e.g., limestone or sandstone). The first two permeable materials (porous sediments and fractured bedrock) have been encountered by a water well drilled at the St. Francis of Assisi Catholic Secondary School (formerly known as Vanier Catholic Secondary School) in the Riverdale subdivision. This well intersected the Selkirk aquifer (55–60 m deep, ~25 L/sec flow rate, and ~6 deg°C fluids in sand and gravel) as well as the Miles Canyon basalt aquifer (60–143 m deep, ~11 L/sec, and ~7°C in fractured basalt). Both aquifers were considered for a heat pump project (Gartner Lee Limited, 2003). The third potentially permeable rock types mentioned above (limestone and sandstone) are present at the surface and beneath the City of Whitehorse. However, the porosity and permeability of these rock units are poorly understood. Similarly, any subsurface permeability associated with the copper-gold-silver skarn mineralization in the Whitehorse copperbelt is not known.

The presence of warm springs as well as the encouraging drilling results in Riverdale suggest that further investigation to find more geothermal aquifers in the Whitehorse area is merited. However, the exact location, depth and thickness of additional permeable rock units in the region is currently not known. Likewise, little is known about fault structures in the area, that may or may not act as permeable conduits to allow geothermal fluids to ascend from greater depths.

The goals of this study are to obtain and interpret baseline geoscience data in the Whitehorse area to:

- Develop a 3D geologic framework for the Whitehorse subsurface to better understand the geometry of major rock units and fault structures that may or may not host geothermal reservoirs; and
- Better constrain the thickness of the sedimentary overburden (i.e., depth to bedrock);

The study area for this project is 13 km wide and 15 km long centred around the northern part of the City of Whitehorse (Fig. 2). Existing, public domain geoscience data were compiled for the study area which included: topography, heat flow data, aeromagnetic data, Curie point depth data, radiogenic heat production data, warm springs data, bedrock geology and faults, surficial geology, earthquake data, rock property data and water well data. A new gravity dataset was also collected as part of this project. These datasets are described in this report.

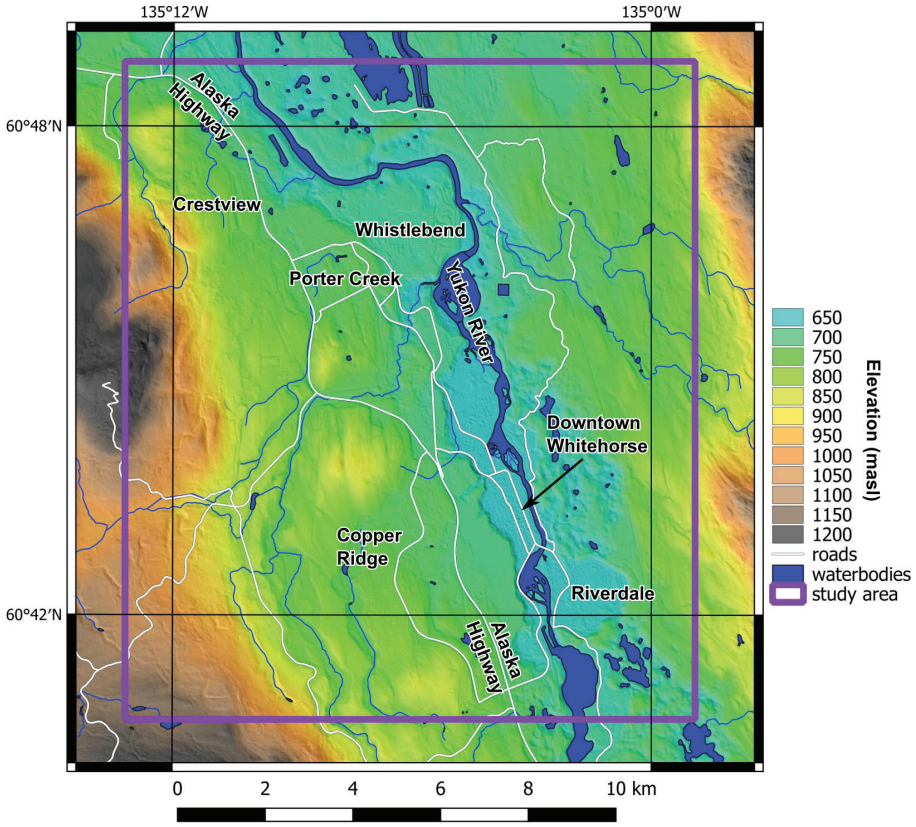

Figure 2. *Topography in the Whitehorse area from Arctic DEM data with the 13 x 15 km study area outlined in purple.*

Background

Typical indicators of high temperature geothermal resources (e.g., boiling springs, steam vents, and active volcanism) are absent within the study area. However, there is geoscience evidence which is relevant to the question of the favourability of geothermal resources in the Whitehorse area. Background information is summarized here.

Curie point depth estimate

Curie point depth mapping has been used as an initial exploration tool in the Yukon to help identify warm vs. cool crustal temperatures in the territory (Witter et al., 2018; Gaudreau et al., 2019). Curie point depth mapping is a geophysical method, which uses regional-scale magnetic survey data to map the depth to the Curie point temperature (~580°C) where magnetization in rocks disappears. Regions found to have shallow CPD values are expected to have higher heat flow, higher average thermal gradient, and therefore, a higher likelihood of geothermal energy resources at shallower depths. Two different CPD values have been estimated for the Whitehorse area in separate studies: ~13.7 km (Li et al., 2017) and ~12 km (Gaudreau et al., 2019). These values translate into an average, crustal-scale temperature gradient of ~42 to 48°C/km. Such a thermal gradient is higher than the average thermal gradient for continental crust (~25°C/km).

Bedrock and surficial geology

Bedrock geology in the Whitehorse area (Fig. 3) can be summarized as follows (from Wheeler, 1961; Hart and Radloff, 1990; Hart, 1997a, 1997b; Yukon Geological Survey, 2023b):

- Quaternary sediments: unconsolidated glacial sediments (sand, clay, gravel);
- Miles Canyon basalt: Miocene to Pliocene columnar jointed olivine basalt (dated 2.4–8.4 Ma);
- Haeckel Hill pluton: Eocene granite (dated 54 Ma);
- Whitehorse batholith: mid-Cretaceous granodiorite and quartz diorite (dated 113 Ma);
- Richthofen formation: Lower to Middle Jurassic turbiditic sandstone-siltstone-mudstone and conglomerate (part of the Laberge Group);
- Mandanna member: Upper Triassic greywacke, pebble conglomerate, and mudstone (part of the Aksala formation in the Lewes River Group);
- Hancock member: Upper Triassic massive to thick-bedded limestone (part of the Aksala formation in the Lewes River Group);
- Casca member: Upper Triassic shale, siltstone, greywacke, and limestone (part of the Aksala formation in the Lewes River Group);
- Povoas formation: Upper Triassic augite or feldspar-phyric andesitic basalt flows, breccia, tuff, sandstone, and argillite (part of the Lewes River Group).

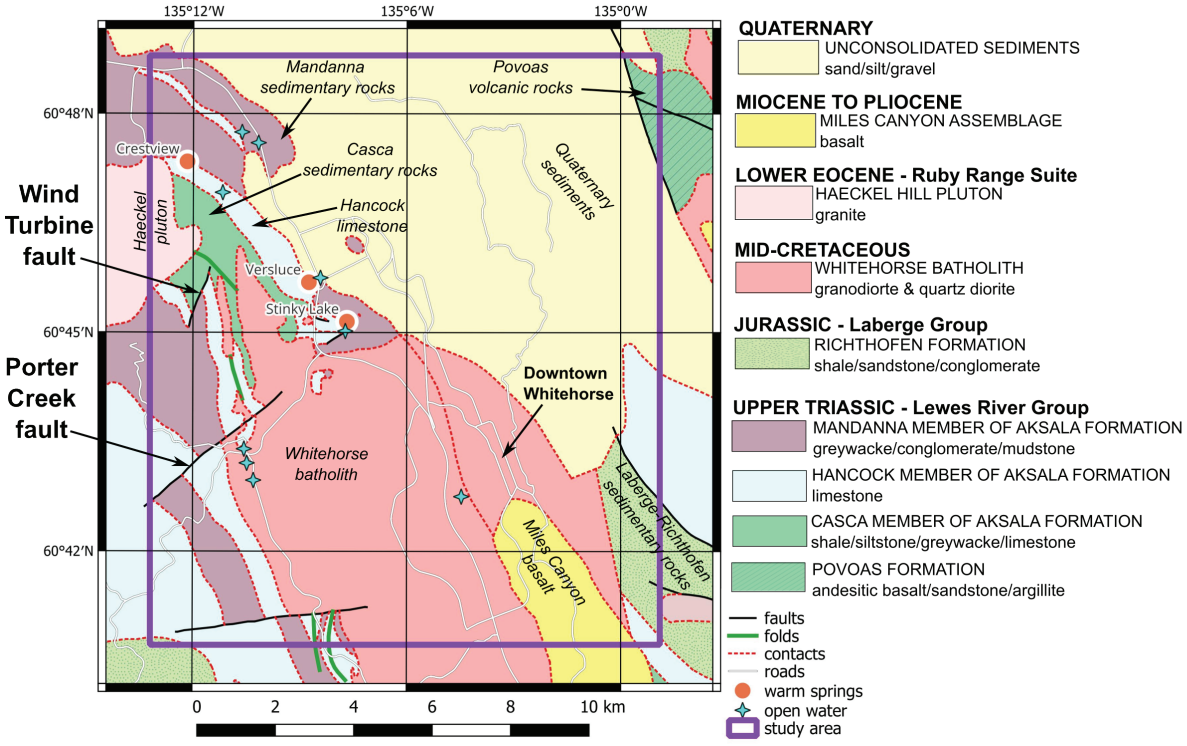

Figure 3. *Bedrock geology for the northern part of the City of Whitehorse, Yukon (adapted from Yukon Geological Survey, 2023b). Major rock types are identified and described in the legend. Locations of warm springs (orange dots) and stretches of open water observed in winter (turquoise stars) are indicated. The study area is outlined in purple. Fault names are informal and were chosen for this study.*

Surficial geologic mapping (Bond et al., 2005a, 2005b, 2005c; Lipovsky, 2023) shows that the Whitehorse area is blanketed by significant thicknesses of glacial sediments deposited during the McConnell Glaciation (~20 000 years ago) which have since been incised by the Yukon River and its tributaries. In the central part of the study area (i.e., downtown Whitehorse), much of the glacial material consists of fine-grained sediment deposited on the floor of Glacial Lake Laberge during the last Ice Age. In other areas, the glacial sediments are dominated by glaciofluvial material and till. Bedrock is not exposed across most of the study area, but it is found in upland regions and other areas that have been scoured by glaciers.

Geologic structures

Major faults in the greater Whitehorse area include:

a) Braeburn fault – a large-scale, NNW-trending, dextral strike-slip fault that lies a few kilometres NE of the study area.

b) Ibex thrust fault – a N-S trending thrust fault the lies ~15 km west of the study area.

Three faults have also been mapped within the study area near the western margin of the Whitehorse batholith. These faults trend E-W to NNE-SSW (Fig. 3). None of these faults show evidence of recent movement (Lipovsky, 2023).

A NW-trending anticline is present in the sedimentary rocks of the Aksala formation in the NW quadrant of the study area (Fig. 3). This fold is defined by bedrock mapping (i.e., older rocks are found in the core of the fold and younger rocks on the limbs) and sparse structural measurements that record a dip angle on the limbs of the fold of 20 to 30° (Hart et al., 1997a; Yukon Geological Survey, 2023b). Gentle folding is also present in Aksala formation rocks on the SW edge of the study area.

Volcanism and warm springs

About 8.4 million years ago volcanic rocks erupted from a vent on the flank of Golden Horn Mountain located ~15 km south of downtown Whitehorse. Lava from this eruption flowed north to reach the SE corner of the study area (Fig. 3). These mafic volcanic rocks are now known as Miles Canyon basalt and they are dominated by columnar-jointed lava and associated scoria with individual flows up to 20 m thick (Hart and Villeneuve, 1999; Pearson et al., 2001). Additional mafic rocks at the Alligator Lake volcanic complex, located ~30 km SE of the study area, erupted between 6.8 and 3.1 Ma. The magma that served as the source for these volcanic rocks likely cooled long ago and is, therefore, not a heat source for a modern-day geothermal system.

Warm springs located on the NW side of the study area have surface discharge temperatures of 18.5°C (Stinky Lake), 12.7°C (Versluce) and 12°C (Crestview) (EBA Engineering Consultants Ltd., 2009; Yukon Geological Survey, 2024). These warm springs occur over a distance of ~6 km at the geologic contact between the Hancock limestone and Mandanna sandstone units (Fig. 3). This suggests that the rock along this geologic contact may be permeable and play an important role in allowing the geothermal fluids to come to the surface.

Stinky Lake warm spring is located 20 m west of the lake of the same name. The flow rate out of the spring is estimated as 1 L/sec (EBA Engineering Consultants Ltd., 2009) and there is a hydrogen sulfide smell in the area. The Versluce warm spring is located west of the Porter Creek subdivision near the NE side of the Whitehorse landfill. The flow rate is estimated to be a few litres per second (EBA Engineering Consultants Ltd., 2009) and the water is odourless. The Crestview warm spring is located in a wetland ~2 km west of the Crestview subdivision

on the NW side of Whitehorse. Flow rate from the Crestview warm spring is <1 L/sec and the water is odourless.

As part of a Yukon Geothermal Exploration Program (EBA Engineering Consultants Ltd., 2009; EBA Engineering Consultants Ltd., 2010a, 2010b; EBA, A Tetra Tech Company, 2011a, 2011b), chemical analysis of water samples collected from the three warm springs yielded the following information:

- The spring waters are classified as calcium-magnesium-bicarbonate type, which suggests an origin in sedimentary, carbonate-rich rocks.
- All spring water samples have a similar chemical composition, pH and electrical conductivity which suggest a similar origin (EBA Engineering Consultants Ltd., 2009).
- Water isotopes fall on the 'meteoric line' for the Whitehorse area, which suggests a meteoric (i.e., not magmatic) source for the spring water.
- Tritium isotopes measured in the spring waters suggests a short residence time in the subsurface of less than 50 years.
- $^{3}He/^{4}He$ ratios measured from the waters of Stinky Lake warm spring suggest mantle helium is penetrating through the crust and arriving at the surface (EBA Engineering Consultants Ltd., 2009). The helium ratios at Stinky Lake are similar to several magmatic and deep circulation type geothermal systems in the Great Basin of western USA (Siler and Kennedy, 2016).
- Silica geothermometry analysis of two of the spring water samples gave equilibrium deep aquifer temperatures of 87°C and 54°C for the Stinky Lake and Versluce warm springs, respectively. EBA Engineering Consultants Ltd. (2009) suggests that these estimates are likely minimum temperatures since the amount of mixing with cold shallow ground water is unknown.

These results led EBA Engineering Consultants Ltd. (2009) to conclude that there is a geothermal anomaly underneath the Porter Creek and Crestview subdivisions in Whitehorse that may be the source of all three warm springs.

More regionally, geothermal waters also reach the surface at Takhini Hot Springs (47°C; Fraser et al., 2018; Langevin et al., 2020; Léveillée-Dallaire and Raymond, 2024) located ~24 km NW of Whitehorse and at Vista Mountain Warm Springs (8–14°C; EBA, A Tetra Tech Company, 2012) located ~22 km north of Whitehorse. It is important to note that, similar to the warm springs in Whitehorse, both of these springs occur at or near the geologic contact between the Hancock limestone and Mandanna sandstone rock units.

In addition to the warm springs, open water observed in the Whitehorse area in the winter months is likely indicative of warm geothermal fluids ascending from the subsurface that prevents water at the surface from freezing. Several locations of open water have been identified (Fig. 3; Yukon Geological Survey, 2024). Most are situated in the vicinity of the Hancock limestone, which may suggest elevated permeability in this rock unit. Some of the areas of open water lie along strike of NE and NNE-trending mapped faults which may indicate fracture permeability along these geologic structures.

Shallow well data

Records from ~500 water wells are available for the Whitehorse study area (Yukon Water Well Registry website; https://yukon.ca/en/get-information-about-yukon-groundwater-and-wells).

These water well records can be important because many provide data on: subsurface geology, depth to bedrock and subsurface temperature (Fig. 4). The water wells range in depth from ~1 m to 216 m. Eighty-one of these wells record information on the depth to the top of bedrock (Lipovsky, 2023). The wells that intersect bedrock are important for construction of a depth-to-bedrock map for the Whitehorse area that forms a key part of this study.

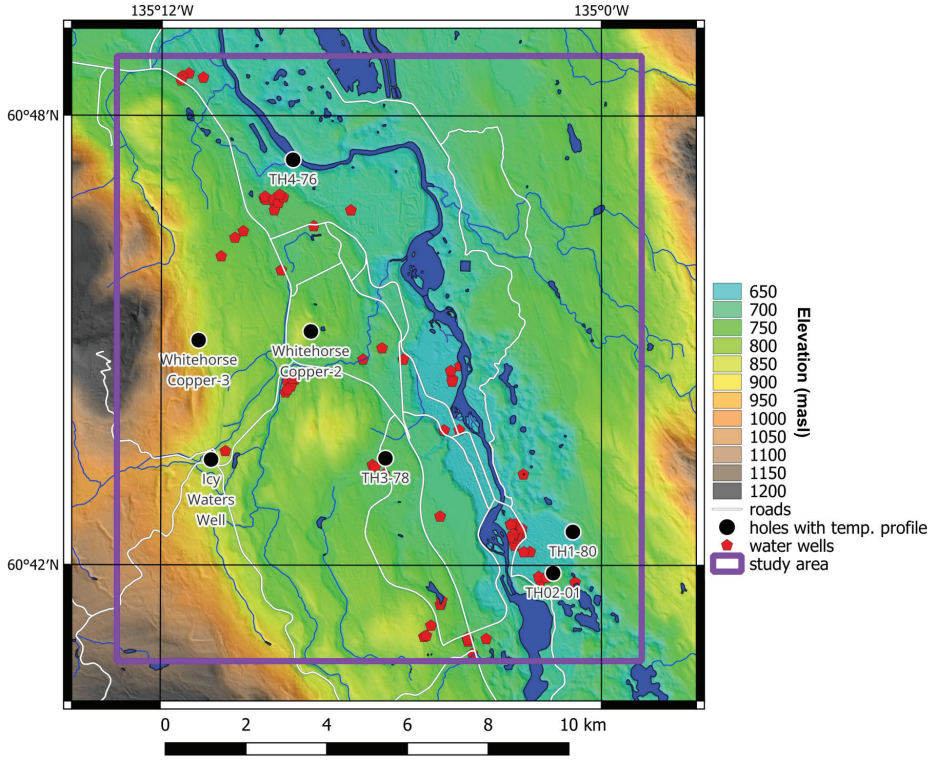

Figure 4. *Locations of 81 water wells with depth-to-bedrock information (red pentagons). The black dots indicate boreholes which have downhole temperature profile data shown in Figure 5.*

Downhole temperature profile data has been recorded at eight holes drilled in the Whitehorse area (Fig. 5). These data reveal highly variable subsurface temperatures at depth across the area. Three examples are:

- Whitehorse Copper-3 mineral exploration borehole reached a modest temperature of ~8°C at a depth of 336 m
- TH02-01 water well in the Riverdale subdivision reached a slightly higher temperature of ~9°C at a much shallower depth of only 145 m in the Miles Canyon Basalt Aquifer
- TH4-76 water well reached a temperature of 4.5°C relatively near the surface at a depth of only 36 m

The average subsurface temperature gradient has been calculated for the three wells mentioned above and the results are described here (Fig. 5). The Whitehorse Copper-3 well has a linear temperature profile with an overall average gradient of only ~20°C/km, which is lower than the global average temperature gradient for continental crust (25°C/km). The linear profile suggests that no aquifers were encountered. In contrast, the overall average temperature gradient at the TH02-01 well is ~37°C/km, about twice as high as the Whitehorse Copper-3 well. The non-linear features in the temperature profile from the

TH02-01 well reflect different aquifers at different temperatures encountered in the well. Lastly, the temperature profile at well TH4-76 is also linear but the gradient has an unusually high value of 62°C/km. The TH4-76 well was drilled into glacial sediments, is very shallow (36 m), and the bottom hole temperature is only 4.5°C. Since background shallow groundwater temperatures in the Whitehorse area are reported to be 2 to 5°C, without a deeper well, it is difficult to know if well TH4-76 simply encountered typical groundwater or if the surprisingly high temperature gradient is indicative of higher temperatures at even greater depths. Notably, subsurface temperatures measured in glacial sediments in wells near Haines Junction, Yukon, yielded elevated temperature gradient values 56–68°C/km (Witter, 2024) similar to the TH4-76 well. More subsurface temperature measurements from deep wells are needed in the Whitehorse area to answer this question.

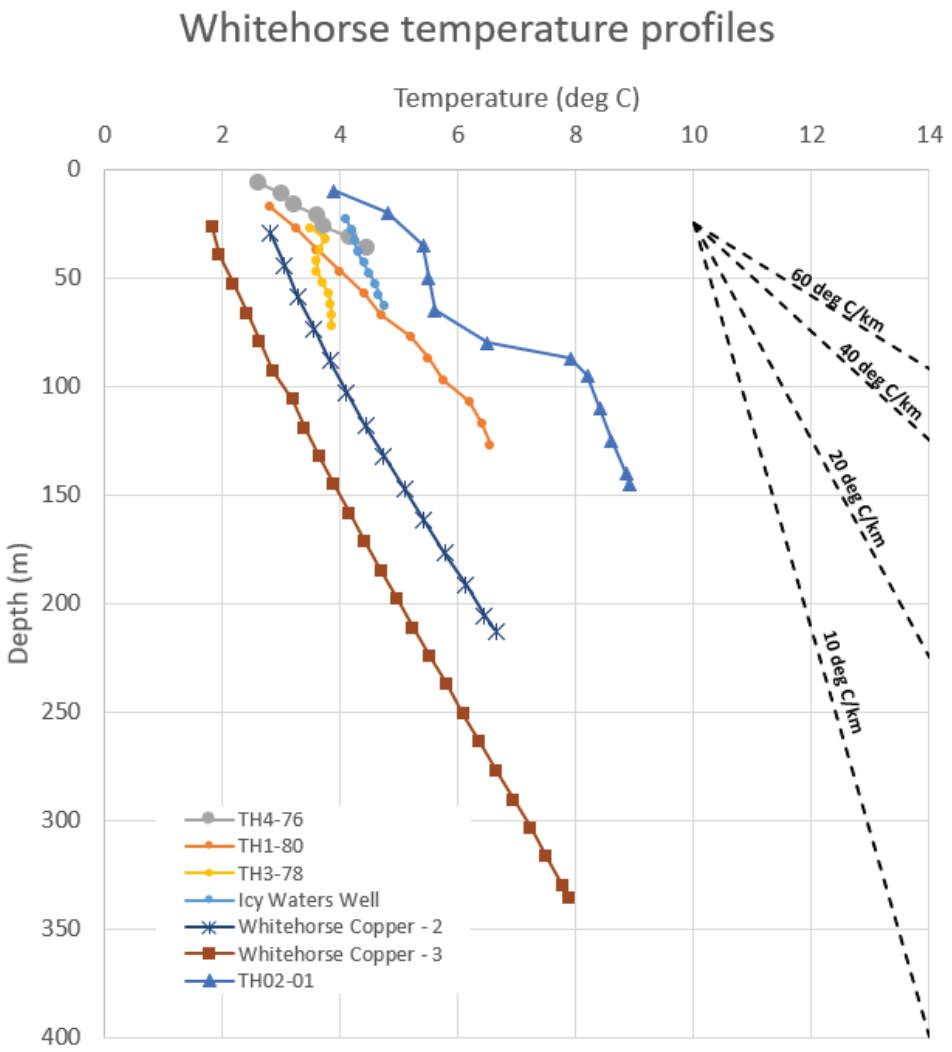

Figure 5. *Temperature profiles from Whitehorse area wells and boreholes (adapted from EBA Engineering Consultants Ltd., 2008).*

Deep well data

According to public records, only one deep well (i.e., >500 m) has been drilled in this part of the Yukon. Approximately 11 km south of downtown Whitehorse, the North Star well was drilled in 2012 as test hole to a depth of 2000 m. Downhole temperature profiles were

measured three times (to depths of 640, 1050 and 1414 m) and returned temperature gradients of 25-28°C/km (Yukon Geological Survey, 2024). The North Star well was drilled into the granitoid rocks of the Whitehorse batholith (Yukon Geological Survey, 2023b).

Heat flow data

One heat flow measurement of 60 mW/m^2 is reported by Lewis et al. (2003) for Whitehorse. This heat flow measurement was obtained from the Whitehorse Copper-3 borehole which also has a low temperature gradient (Fig. 5). The reported heat flow value is similar to the mean heat flow for continental crust (65 mW/m^2) but it is significantly lower than regional heat flow measurements for southern Yukon (Lewis et al., 2003) that are on the order of ~80–100 mW/m^2.

Radiogenic heat production data

There are many direct estimates of radiogenic heat production from plutons located in the region around Whitehorse (Colpron, 2019). Ten samples of rocks from the Whitehorse batholith returned values of 1.2 to 2.9 µW/m^3 which are similar to or less than the global average value for heat production in granites (2.5–2.8 µW/m^3; Hasterok and Webb, 2017). In contrast, seven samples from the Haeckel Hill pluton, located NW of the city, gave higher heat production values of 2.9 to 5.0 µW/m^3 (Yukon Geological Survey, 2024). Based upon these data, radiogenic heat production may be a significant heat source for geothermal reservoirs in the vicinity of the Haeckel Hill pluton but not near the Whitehorse batholith.

Earthquake data

Data on earthquake epicenters for the Whitehorse area were obtained from the U.S. Geological Survey Earthquake Catalog website (https://earthquake.usgs.gov/earthquakes/search/) by searching for all earthquakes from 1900 to December 2024. No historic earthquakes are reported within the Whitehorse study area and only two were reported nearby, both at a distance of ~20 km from the study area. These two quakes occurred in 2012 and 2023 with magnitudes of 1.5 and 2.5, respectively, and depths >6 km. One of these quakes is located along strike of the Braeburn fault and the other is positioned near the Ibex thrust fault. The lack of earthquakes suggests that fractured, permeable rock in the subsurface caused by active fault motion is not likely present within the Whitehorse study area.

Favourable geothermal environments

For geothermal fluids to flow underground, there needs to be porosity and permeability in the rocks either in the form of faults and fractures, permeable geologic contacts or natural pore space.

Studies from southern Yukon show that the tectonic regime in the area is under compression in a direction oriented approximately NE-SW (Hyndman et al., 2005). Such conditions in the crust tend to close geologic structures that are oriented perpendicular to the compression direction (i.e., NW-SE striking structures). However, NE-SW oriented structures that run parallel to the compression direction are more likely to be permeable.

Multiple fault structures cut the western side of the Whitehorse batholith. In the south, faults that cut the Whitehorse batholith are oriented E-W. However, at the north end of the Whitehorse batholith, two faults are mapped with NE-SW (Porter Creek fault) and NNE-SSW strikes (Wind Turbine fault; Fig. 3). Both of these faults are more likely to be permeable

than faults with other orientations. Indeed, the mapped end of the Porter Creek fault lies only ~200 m from the Stinky Lake warm spring which suggests a possible relationship.

Geologic contacts between rock units may also have favourable permeability based upon their orientation with the regional compression direction. For example, the northern and southern margins of the radiogenic Haeckel Hill pluton are oriented in a NE-SW direction that may be favourable for permeability. In contrast, the three warm springs in the Whitehorse area are all situated along the Hancock limestone – Mandanna sandstone geologic contact which is oriented NW-SE. This orientation is perpendicular to the regional tectonic compression direction and, therefore, less favourable. This suggests that the geologic contact itself may not be permeable and that the permeability that allows geothermal fluids to ascend to the warm springs may have a different origin.

Naturally porous and permeable rocks make excellent geothermal reservoirs. Wells drilled into the Miles Canyon basalt unit have already shown that it is porous, likely due to a combination of the natural fractures that formed when the basalt lava cooled, and volcanic breccia associated with lava flow emplacement. The porosity of the two rock units that flank the three warm springs (Hancock limestone and Mandanna sandstone) is not known. The porosity of the Quaternary glacial sediments that cover the Whitehorse area varies from clay-rich non-porous material to sand/gravel-rich, high porosity layers.

Geothermal exploration summary and strategy

What do we know?

Existing geoscience information in the study area, outlined in the previous section, suggests the following:

- An above average crustal thermal gradient of ~42 to 48°C/km could be present in the Whitehorse region, based upon CPD mapping.
- Active volcanism occurred 8.4 Ma just south of the study area and erupted the Miles Canyon basalt. The magma that remains in the crust from this eruption has likely cooled and solidified since then.
- Downhole temperature data from wells and boreholes in the area show highly variable temperature gradients from 20 to 28°C/km deep in the Whitehorse batholith, to ~37°C/km in the Miles Canyon basalt, and to 62°C/km at shallow levels in the glacial overburden.
- Three warm springs reach the surface along the geologic contact between Hancock limestone and Mandanna sandstone, geologic relations that are similar to those found at Takhini hot springs and Vista Mountain warm springs.
- Surface discharge temperatures of the Whitehorse area warm springs are 12.0 to 18.5°C but silica geothermometry of the analysed spring water suggest minimum geothermal reservoir temperatures of 54 to 87°C.
- Heat flow measured in a well in the Whitehorse batholith is unusually low compared to regional heat flow measurements across southern Yukon.
- Radiogenic heat production from the Whitehorse batholith is less than the global average. However, for the Haeckel Hill pluton, the measured radiogenic heat production is higher than the global average.
- Two mapped faults in the study area, that strike NE-SW and NNE-SSW, are

favourably oriented with respect to the regional tectonic compression direction. One of these faults terminates near a warm spring. Open water in winter is observed along strike of these faults.

- Faults in the study area show no evidence of recent movement.
- Except for two events outside the study area, recent earthquake activity is absent and our understanding of fault-related fracture permeability in bedrock in the study area remains limited.
- Geologic mapping and water well data shows that the area is blanketed by glacial sediments that vary in thickness from zero to hundreds of metres thick.

What do we want to know?

The two key requirements for a viable geothermal resource are elevated temperature and adequate rock permeability. Downhole temperature data from the Whitehorse area suggests that the thermal gradient in the subsurface depends on location and may be dependent on rock type with boreholes drilled into the Whitehorse batholith giving low temperature gradient values. Unfortunately, all the wells drilled outboard of the Whitehorse batholith are quite shallow (i.e., <200 m). As a result, deeper temperatures in the vicinity of the warm springs and elsewhere are poorly known. Similarly, silica geothermometry gives estimated minimum temperatures of the reservoirs beneath the warm springs but the actual geothermal fluid temperatures have not yet been measured. Are the actual reservoir temperatures higher? If so, how much? Drilling of additional temperature gradient wells will be required to help answer these questions.

Radiogenic heat production data shows that the Haeckel Hill pluton may be a source of heat for nearby geothermal aquifers. But what exactly is the relationship between the Haeckel Hill pluton and the warm springs? What, if any, is the geothermal fluid flow path from this pluton to the warm springs?

The elevated shallow temperature gradient in well TH4-76 located in the glacial sediments is encouraging. But does it point towards warm geothermal aquifers in the porous sand and gravel sections of the glacial sediment pile? If so, how deep do these porous aquifers reside? This is important because the hottest, sediment-hosted geothermal aquifers are found in the deepest portions of the sediment pile, at or near the contact with the top of bedrock. Alternatively, does the elevated temperature gradient measured in well TH4-76 continue deeper into bedrock?

In order to begin to address these questions, a more thorough understanding of the 3D geologic framework of the subsurface is required. Thus, a significant amount of the effort in this study is aimed at building a 3D geoscience model of the lithology and faults within the project area as well as a depth-to-bedrock map showing the thickness variations of the glacial sediments. The overall goal is that the 3D geoscience model will serve as a guide for selecting drilling targets that would give direct characterization of the bedrock as well as measurements of subsurface temperature and permeability. The next sections describe the data and methods used to create a 3D geoscience model that is consistent with geoscience datasets used in this study.

Data used in this project

Existing geoscience data

Topographic data

Topographic data compiled in the Whitehorse area include Arctic DEM data (as good as 2 m resolution) and lidar data (as good as 1 m resolution; Aurora Geosciences Ltd., 2024). To create the best possible topographic dataset for the study area, the lidar data was prioritized everywhere it was available and supplemented by Arctic DEM data, as needed. Elevation in the Whitehorse study area ranges from ~600 m above sea level (asl) in the Yukon River bottom to ~1400 masl in the mountains to the west (Fig. 2).

Surficial geology data

Surficial geologic maps are particularly valuable for this study because they document where bedrock does and does not outcrop at the surface. This information helps to determine the thickness variations of the glacial sediment cover. Detailed surficial geologic mapping (Lipovsky, 2023) divided the land surface into terrain units based upon the composition of the surficial materials. Each mapped terrain unit that contains a portion designated as 'bedrock' can be considered as a region with relatively thin sediment cover (or near-zero depth-to-bedrock, Fig. 6).

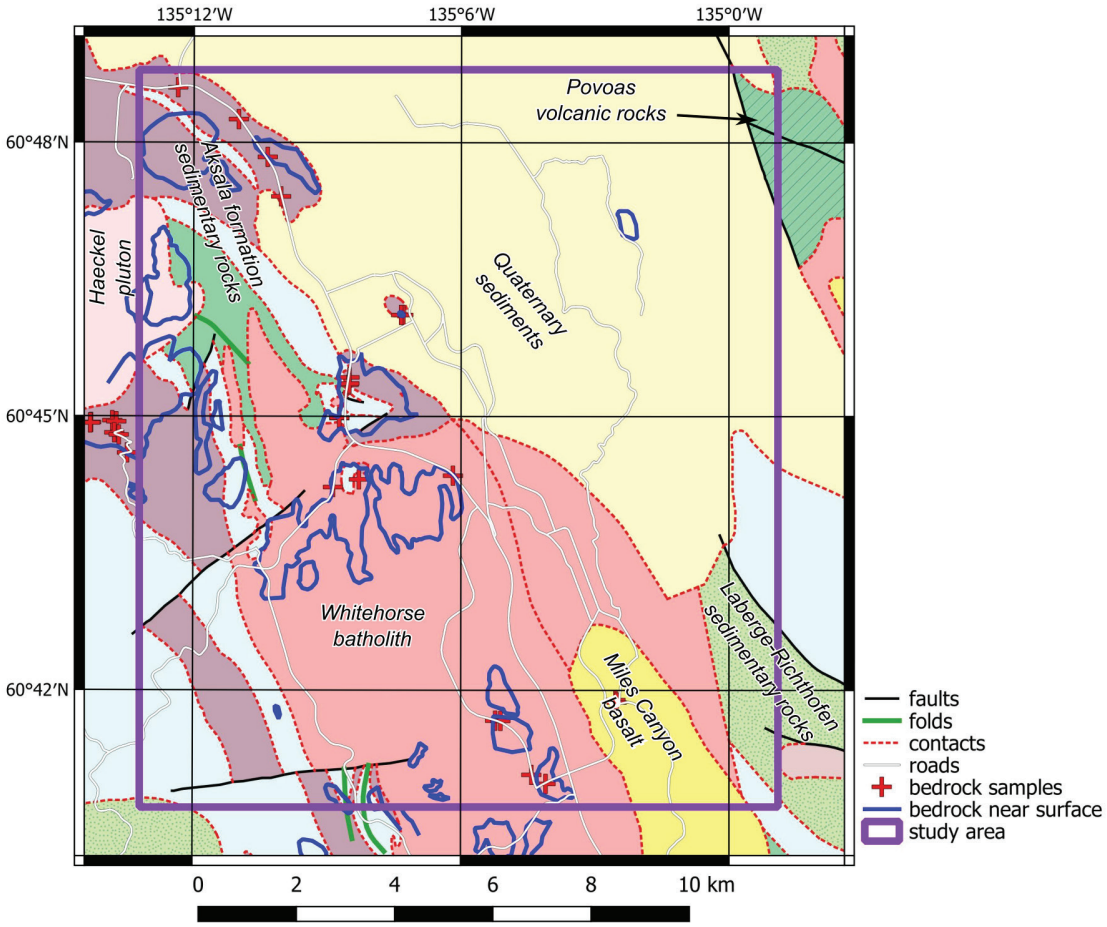

Figure 6. *Map showing the terrain units of Lipovsky (2023) that contain bedrock (dark blue polygons). Locations of samples of bedrock collected for rock properties are also shown (red crosses). Bedrock geology map (Figure 3) is shown in the background.*

Airborne magnetic survey data

Magnetic survey data were obtained by the Geological Survey of Canada for the Whitehorse area. These data are part of a larger Yukon compilation that consists of multiple airborne surveys that were re-processed and re-gridded (Aurora Geosciences Ltd. and Bruce, 2020). In the Whitehorse area, however, these magnetic survey data are quite coarse, composed of data points collected in aeromagnetic surveys from 1961 and 1966 along lines spaced ~1.5 km apart (Fig. 7). These regional-scale data were used for both the map-based interpretation and the 3D magnetic inversion modelling in this study. High-resolution magnetic survey data were acquired by Gladiator Metals Corp over about 30% of the western portion of the study area and made available for comparison with the regional-scale magnetic survey data.

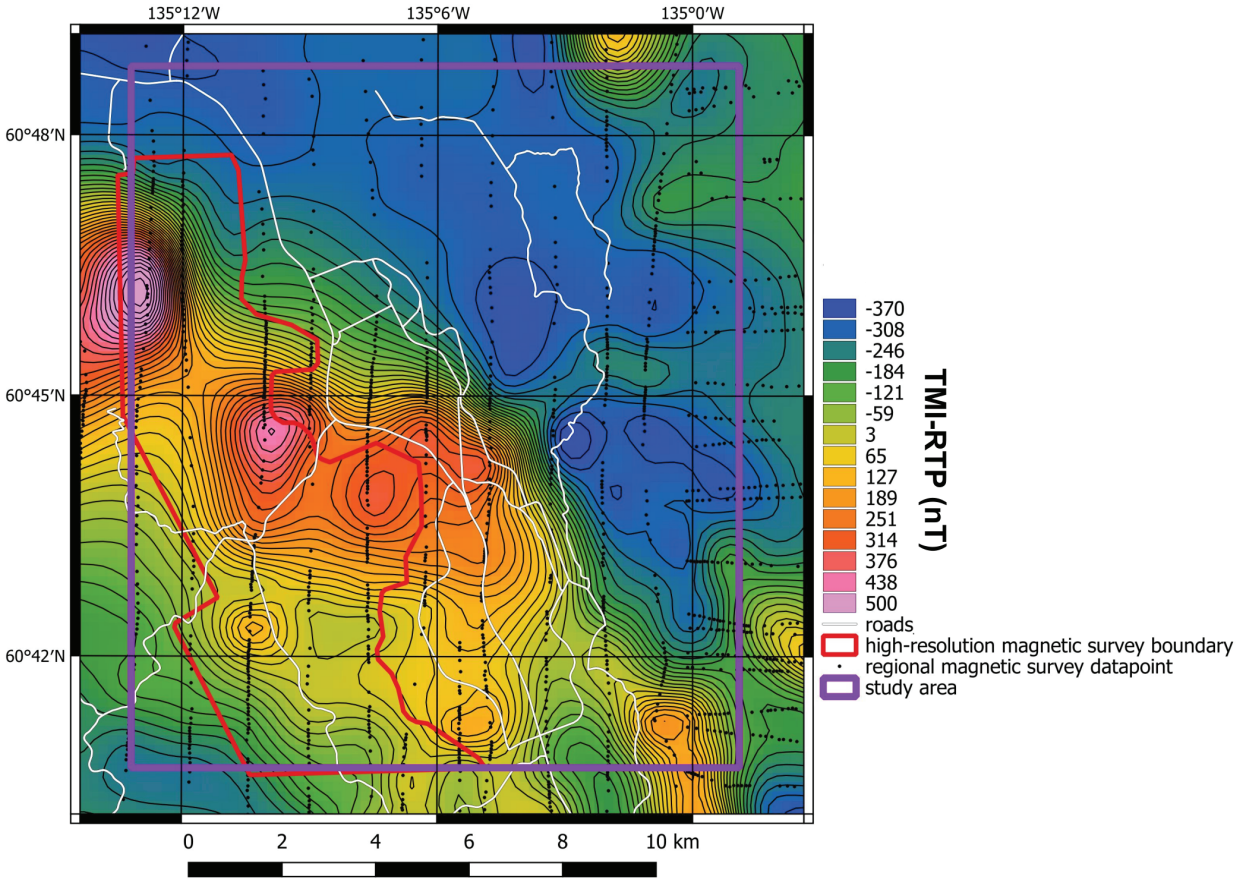

Figure 7. *Public domain, regional-scale magnetic survey data for the Whitehorse area plotted as Total Magnetic Intensity – Reduced to Pole (TMI-RTP). The aeromagnetic survey data points from the 1960's that were used to construct this map are shown as black dots and lay along survey lines spaced ~1.5 km apart. The cool/warm colours in the map represent magnetic lows/highs. The study area is shown by the purple rectangle. The red polygon shows the area where high-resolution magnetic survey data were made available for this study (actual high-resolution data not shown).*

Newly collected geoscience data

Gravity survey data

Gravity data are useful to improve understanding of the geometry of rock units and depth to bedrock. In 2023–2024, Aurora Geosciences collected new gravity measurements at 450 stations over an irregularly shaped ~12.5 by 10.0 km survey area using 500 m station

spacing (Fig. 8). The gravity survey was conducted in two phases with the first phase covering the northern area and the second phase covering the southeastern part. A region in the SW corner of the study area was not covered with gravity stations due to time and budget constraints. High-resolution GNSS (Global Navigation Satellite System) elevation measurements were made at each gravity station. Gravity stations were not collected over water bodies (i.e., Yukon River) or at the Whitehorse airport due to access issues. The overall measurement error for the gravity survey is estimated at 0.05 mGal. A full description of both phases of the gravity data acquisition by Aurora Geosciences Ltd. is in Appendix A.

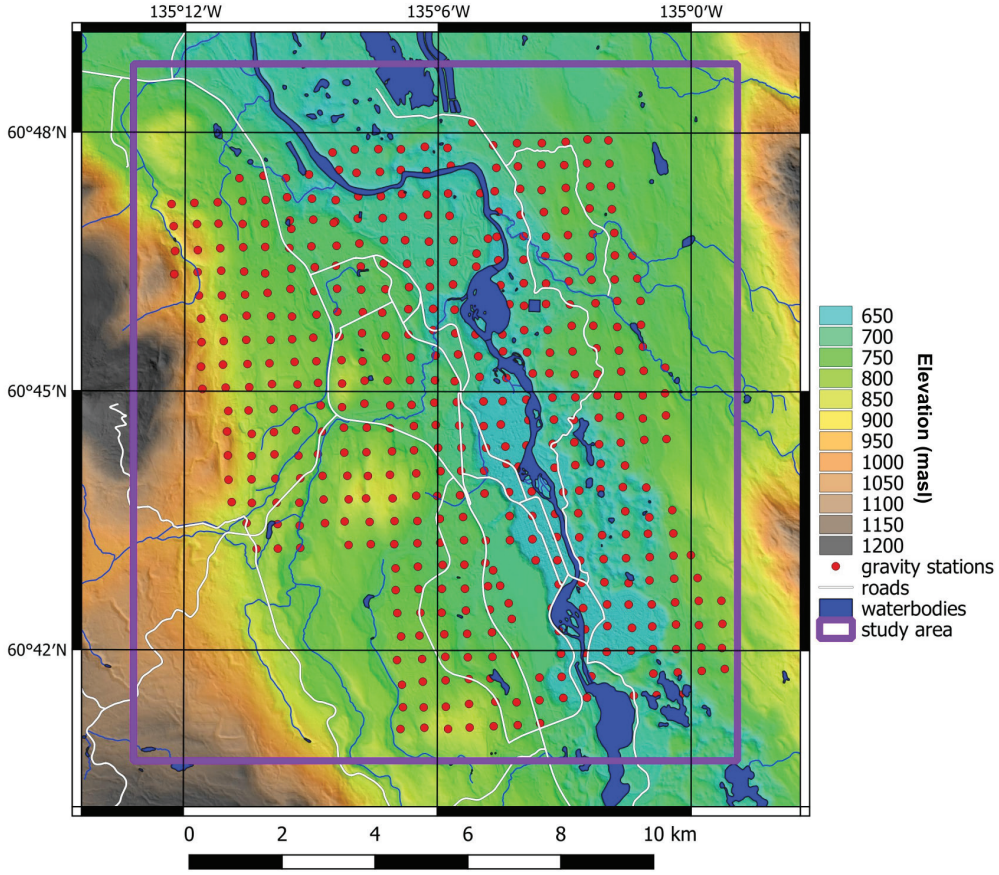

Figure 8. *Map showing gravity stations (red dots) occupied in the 2023-2024 gravity survey by Aurora Geosciences Ltd. The study area is indicated by the purple rectangle. The gravity survey area does not cover the entire study area due to time and budget constraints. The background image shows topography, waterbodies and roads.*

Magnetotelluric survey data

As part of this project, the Yukon Geological Survey and the Geological Survey of Canada contracted Quantec Geoscience Limited in 2022–2023 to conduct a regional-scale magnetotelluric (MT) survey in southern Yukon to better understand electrical resistivity variations in the subsurface. A handful of these MT stations were deployed within the Whitehorse study area with a nominal station spacing of 10 km. These geophysical data have not yet been incorporated into the present study because resistivity modelling of the MT data is still underway at the time of writing.

Methodology

Map-based interpretation

To better characterize the structural and geologic framework within the study area, the following data sets were interpreted using a map-based approach: topography, gravity, magnetics and geology. All map-based interpretation was performed using QGIS software (qgis.org).

Various filters were applied to the gravity and magnetic survey data to aid map-based interpretation of the spatial extent of dense and magnetic rock units as well as the orientation of inferred fault structures that may lie under sedimentary cover. These filters include: first vertical derivative, total horizontal gradient, and tilt derivative, as well as analytic signal (magnetics only). Geophysical filtering was performed using Geoscience ANALYST Pro software (https://mirageoscience.com/). The gravity and magnetic geophysical data were interpreted in conjunction with the mapped geology (e.g., Yukon Geological Survey, 2023b) and rock properties to better understand the geophysical response of the major rock units in the study area.

2D gravity profile modelling

In order to aid with the depth-to-bedrock modelling, several 2D profile models were constructed across the study area using gravity data. These models were constructed with FastGrav software (http://fastgrav.com/). The bedrock units in the models were assigned density values based on rock property measurements of hand samples and the geometries of the bedrock units were estimated from an initial 3D geologic model built as part of this study. A density of 2.0 g/cm3 was assumed for the Quaternary sediments. The sediment thickness was then varied along the profile until the gravity response of the model matched the measured gravity data. The purpose of this exercise was to obtain rough estimates of the potential variation in thickness of the sediment cover along specific transects. The individual top-of-bedrock models derived from the 2D profiles were then interpolated to make a rough 3D top-of-bedrock surface which was then further refined in the 3D geology modelling.

3D geology modelling

Three-dimensional geologic models were constructed for the study area to aid in interpretation and to serve as an important guide for 3D gravity and magnetic inversion modelling. Rhinoceros software (www.rhino3d.com) was used to build the 3D geologic model as surfaces that represent geologic horizons and faults. The 3D geologic model was built to honour the bedrock geology map, surficial geology map and water well data as much as possible. Geologic contacts of the plutonic rock bodies were assumed vertical.

3D gravity modelling

Three-dimensional geophysical inversion modelling of gravity data was performed as part of the effort to iteratively build a 3D geologic framework for the project area. Gravity data are sensitive to changes in subsurface rock density and rock density can be used as a proxy for rock type, provided sufficient density contrasts between rock units are present. The 3D inversion modelling of gravity data pursued here was guided by both the 3D geologic model described above as well as average rock density values for each geologic unit. The inversion algorithm employed for the modelling is the open source SimPEG code (Cockett et al., 2015). We used

both rock property and geologically-constrained inversion strategies as described by Fullagar and Pears (2007) and Fullagar et al. (2008). In addition, we used spatially variable mixed Lp norms for the model regularization as described in Fournier and Oldenburg (2019).

The 3D gravity model volume has the following dimensions: 13 km E-W x 15 km N-S x 4 km thick. We assumed a background rock density value of 2.67 g/cm^3. The 3D model mesh consists of cubic cells of the following sizes: 10 m cells from 0 to 20 m depth and 40 m cells below that. The purpose of the 10 m model cells is to provide detail of the topographic surface. Two kilometres of padding cells were added to the model volume to minimize edge effects. The topographic surface used for the 3D geophysical model volume was derived from lidar DEM data mentioned previously. A total of 444 gravity data points were used in the inversion modelling (six stations were dropped because they did not pass quality control tests). The gravity data consisted of Complete Bouguer Anomaly (CBA) gravity values with a terrain correction density of 2.67 g/cm^3. The gravity data were upward continued by 300 m prior to inversion modelling to minimize near surface effects and model artifacts. The 3D density model derived from the gravity inversion modelling is available in Appendix B.

3D magnetic modelling

Magnetic data are sensitive to variations in the magnetic susceptibility and magnetization direction of rocks in the subsurface. Due to the presence of the magnetic high anomalies spatially associated with the Haeckel Hill pluton and Whitehorse batholith, the initial motivation for 3D geophysical inversion modelling of magnetic data was to help better estimate the geometry of these rock units.

Like the 3D gravity modelling, the 3D inversion modelling of magnetic data was also guided by a 3D geologic model and average magnetic susceptibility values for each rock unit. The magnetic inversion modelling also used the open source SimPEG code (Cockett et al., 2015) and spatially variable mixed Lp norms for the regularization (Fournier and Oldenburg, 2019). To account for magnetic remanence, we employed the magnetic vector inversion algorithm of Fournier et al. (2020) and used normal and reverse values for magnetic declination and inclination as constraints on the modelling. The 3D magnetic model volume is the same size as the one used for the 3D gravity modelling. However, the model mesh consists of 100 m cubic cells. Two kilometres of padding cells were added to the model volume to minimize edge effects.

A total of 7512 magnetic survey data points were used in the inversion modelling, derived from gridded, regional-scale, TMI magnetic survey data from the Yukon Geological Survey (Aurora Geosciences Ltd. and Bruce, 2020). Magnetic field parameters used for the inversion modelling of the regional scale magnetic data include declination (31.4°), inclination (76.6°) and total field strength (58 016 nT). We used a nominal height of 100 m above topography for modelling the re-processed aeromagnetic data.

Magnetic inversion modelling was also performed on the high-resolution magnetic survey data from Gladiator Metals Corp for comparison with the models derived from the regional-scale magnetic data. Magnetic field parameters from July 2024 were used for the inversion modelling of the high-resolution magnetic data and these include declination (18.4°), inclination (75.9°) and total field strength (56 069 nT). We also used a nominal height of 40 m above topography for modelling the high-resolution magnetic data. The 3D magnetic vector inversion models derived from the magnetic inversion modelling are available in Appendix B.

Limitations and uncertainty of 3D geophysical inversion modelling

Most geophysical models are limited by non-uniqueness. That is, multiple competing geophysical models fit the geophysical data equally well, thereby limiting geologic interpretation. In this study, we try to reduce the impact of non-uniqueness on the interpretation by simultaneously considering the geophysical inferences, rock property data, and a geologically-reasonable 3D geology model that honours bedrock geology mapping and water well data.

Results

Rock property data analysis

As part of this project, rock property data were compiled from hand samples in the Yukon Geological Survey archives. The rock samples come from within (Fig. 6) as well as outside the boundary of the study area and represent the types of rock present. In this study, all young sediments (i.e., above bedrock) are assumed to be Quaternary.

The rock property data were categorized according to the major rock unit to which they belong and were graphed as box and whisker plots for better visualization of the data distribution (Figs. 9 and 10). Simple statistics (i.e., maximum, minimum, mean and 1σ standard deviation) were calculated to assess the variation in the results (Table 1). The average rock property values shown in Table 1 are assumed to be representative of each rock unit and, therefore, were used as starting and reference values in the 3D geophysical inversion modelling.

As shown in Figure 9, average rock density is broadly similar for many of the rock units (~2.73 g/cm^3). However, the volcanic rocks of the Povoas formation have a higher average density (2.88 g/cm^3), Haeckel Hill pluton rocks have a lower average density (2.61 g/cm^3), and Miles Canyon basalt rocks have a very wide range in density values which is typical of Cenozoic volcanic rocks that consist of a mixture of high-density lava and low-density scoria. Samples of the Casca member of the Aksala formation are not available to make measurements of the rock density, so we assume that it has the same average density as the other Aksala formation rocks, or ~2.73 g/cm^3. Since many of the density values for individual rock units overlap with the densities of other units it is difficult to distinguish them based upon density alone.

As shown in Figure 10, the Hancock limestone is the least magnetic rock unit in the study area (~$10^{-4.3}$ SI). The Mandanna unit is divided into a weakly magnetic unit on the north side of the study area (Mandanna North, ~$10^{-3.4}$ SI) and a more strongly magnetic (and highly variable) unit on the west side of the study area (Mandanna West, ~$10^{-2.6}$ SI). The Richthofen formation (~$10^{-3.2}$ SI) also has a low magnetic susceptibility similar to Mandanna North. Samples of the Casca member of the Aksala formation are not available to make measurements of the magnetic susceptibility, so we assume that it has the same average magnetic susceptibility as the other Aksala formation rocks, or ~$10^{-3.3}$ SI. The igneous rocks are, on average, more magnetic than the sedimentary rocks in the study area, with the exception of Mandanna West which covers a large range of magnetic susceptibility values and overlaps with the igneous rocks. The Povoas formation and the Whitehorse batholith have the highest average magnetic susceptibility values in the study area (~$10^{-2.2}$ SI). Rocks of the Haeckel Hill pluton and Miles Canyon basalt are slightly less magnetic, averaging ~$10^{-2.7}$ SI.

Reversely magnetized bedrock strongly influences the geologic interpretation of magnetic survey data. Paleomagnetic data from Miles Canyon basalt samples suggest normal magnetization for lavas within the study area and some pockets of reversely magnetized basalt that lie outside of the study area (e.g., Wolf Creek; Hart and Villeneuve, 1999). Volcanic rocks of the Povoas formation erupted during the Carnian stage of the Triassic period (217–229 Ma).

The magnetic polarity timescale for this time range shows many magnetic reversals with reverse polarity conditions present for about half of the time (Ogg, 2012). This suggests that a significant fraction of the rocks of the Povoas formation beneath Whitehorse may be reversely magnetized.

In summary, due to the overlap in susceptibility values, many of these rock units are magnetically indistinguishable from one another. However, leaving out the Mandanna unit, the igneous rocks are clearly more magnetic than the sedimentary units. Rock property data for Quaternary sediments were not available for this study and, thus, the author uses assumed values (Table 1).

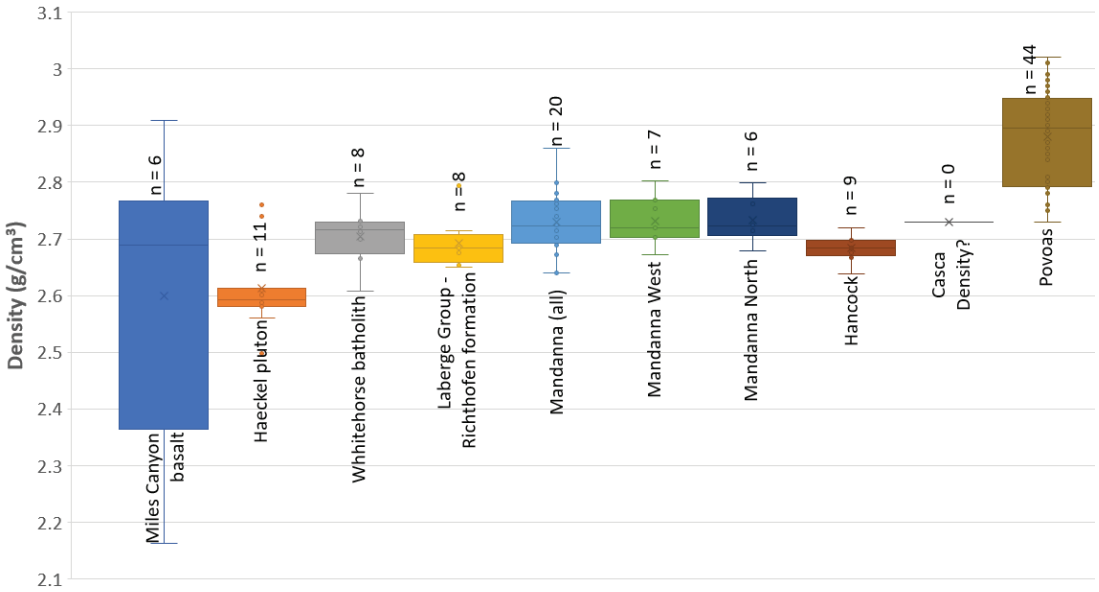

Figure 9. *Rock density data compiled from 106 hand samples that are representative of rock units in the Whitehorse area.*

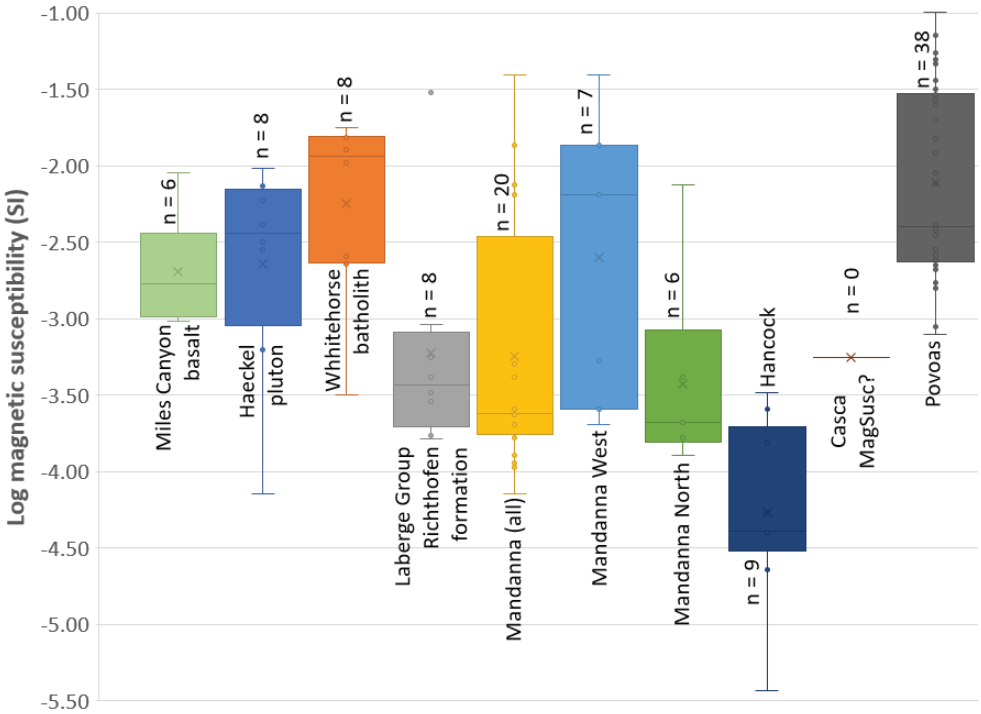

Figure 10. *Rock magnetic susceptibility data compiled from 97 hand samples that are representative of rock units in the Whitehorse area. Variations in magnetic susceptibility are shown on a log scale such that log magnetic susceptibility = -3 is equivalent to a magnetic susceptibility value of 10^{-3} or 0.001 SI units.*

Table 1. *Simple statistics of the A) density data and B) magnetic susceptibility data categorized according to rock type. n = number of measurements. Rock property data for Quaternary sediments are representative values from the literature; those for the Casca member are assumed to be similar to Mandanna.*

a) Rock density data

Rock unit	Minimum (g/cm^3)	Maximum (g/cm^3)	Average (g/cm^3)	1σ Std. Dev. (g/cm^3)	n
Quaternary sediments	n.r.	n.r.	2.00	n.r.	0
Miles Canyon Basalt	2.16	2.91	2.60	0.26	6
Haeckel Hill pluton	2.50	2.76	2.61	0.08	11
Whitehorse batholith	2.61	2.78	2.70	0.05	8
Richthofen formation	2.65	2.79	2.69	0.05	8
Mandanna (all)	2.64	2.86	2.73	0.06	20
Mandanna West	2.67	2.80	2.73	0.04	7
Mandanna North	2.68	2.80	2.73	0.04	6
Hancock limestone	2.64	2.72	2.68	0.02	9
Casca	n.r.	n.r.	2.73	n.r.	0
Povoas formation	2.73	3.02	2.88	0.08	44

b) Rock magnetic susceptibility data

Rock unit	Minimum (Log SI units)	Maximum (Log SI units)	Average (Log SI units)	1σ Std. Dev. (Log SI units)	n
Quaternary sediments	n.r.	n.r.	non-magnetic	n.r.	0
Miles Canyon basalt	-3.0	-2.0	-2.7	0.4	6
Haeckel Hill pluton	-4.1	-2.0	-2.6	0.7	8
Whitehorse batholith	-3.5	-1.7	-2.2	0.6	8
Richthofen formation	-3.8	-1.5	-3.2	0.7	8
Mandanna (all)	-4.1	-1.4	-3.2	0.8	20
Mandanna West	-3.7	-1.4	-2.6	0.9	7
Mandanna North	-3.9	-2.1	-3.4	0.7	6
Hancock limestone	-5.4	-3.5	-4.3	0.6	9
Casca	n.r.	n.r.	-3.3	n.r.	0
Povoas formation	-3.1	-1.0	-2.1	0.6	38

Map-based interpretation

Gravity survey data

The CBA gravity data collected for this study, with a terrain correction density of 2.67 g/cm^3, has the range -119 to -93 mGal (Fig. 11). The key features of the gravity map include:

- A strong gravity high on the NW side of the survey area that coincides with the Haeckel Hill pluton and the Aksala formation rocks.
- A region of moderate-to-low gravity in the NE quadrant of the study area that corresponds to the area mapped as glacial sediments.
- A southern region of moderate-to-low gravity response that correlates to the area

mapped as Whitehorse batholith.

- Relatively low gravity in the area mapped as Miles Canyon basalt.
- A relative gravity high on the eastern edge of the survey area which may represent a bedrock high buried under glacial sediments.

A total horizontal gradient (THG) filter was applied to the gravity data to highlight the zones of greatest horizontal change in the gravity (Fig. 11). The THG filter is commonly used in gravity interpretation to infer fault or rock unit contacts that separate rocks of differing densities. It is possible that faulting could have offset the bedrock vertically to create the observed high/low gravity variations. The Porter Creek fault roughly corresponds to a NE-trending gravity interpretation line (Fig. 12) suggesting that it might be fault-related. However, many of the interpretation lines derived from the gravity data are randomly oriented and likely have little to do with underlying geologic structure. Instead, the interpretation lines inferred from the gravity map most likely represent the edges of shallow bedrock where glacial processes have increased or decreased the amount of sediment cover. In general, the strongest gravity lows likely represent the areas with the greatest thickness of sediment and regions of elevated gravity represent places where bedrock is close to the surface and sediment cover is thin. This interpretation is supported by the surficial geology mapping (Lipovsky, 2023; Fig. 6).

One part of the gravity map which still requires explanation is the gravity high on the western side. This area is dominated by moderate density Aksala formation rocks but the strongest gravity response (Fig. 12) corresponds to the margin of the Haeckel Hill pluton which has a lower density than the adjacent Aksala formation rocks. Higher density rock material is required in this area to create the gravity high. One possible explanation is that contact metamorphism and mineralization on the margin of the Haeckel Hill pluton may have caused precipitation of dense minerals.

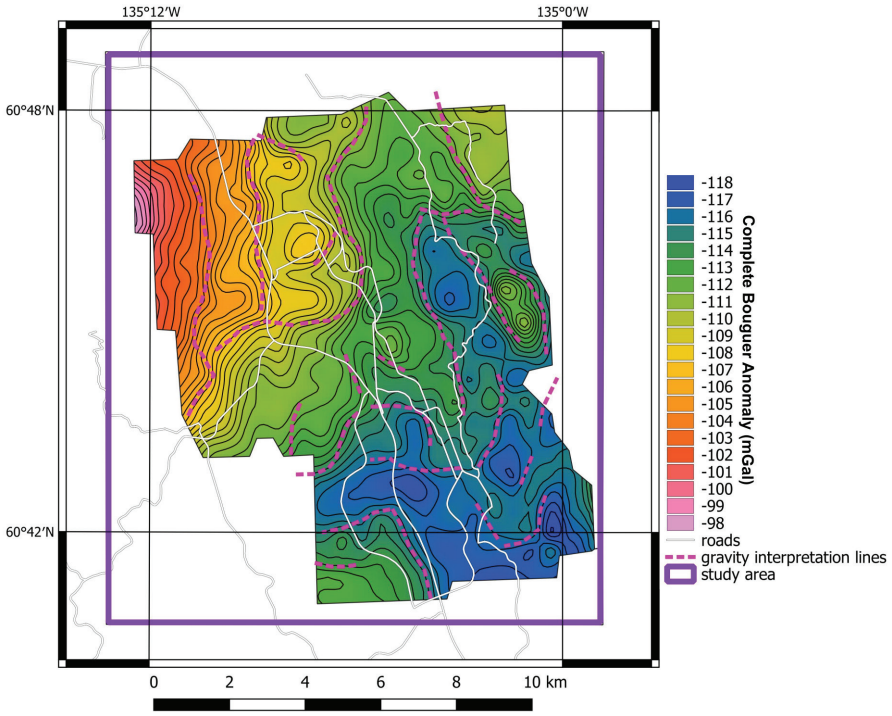

Figure 11. *Complete Bouguer Anomaly (CBA) gravity data gridded with a 100 m cell size. Gravity contours (thin black solid lines) are shown at 0.5 mGal intervals. Cool/warm colours represent gravity lows/highs. Interpretation lines (pink dashed lines) were inferred from another gravity map (not shown) with a Total Horizontal Gradient filter applied (Appendix B). The study area boundary is the purple rectangle.*

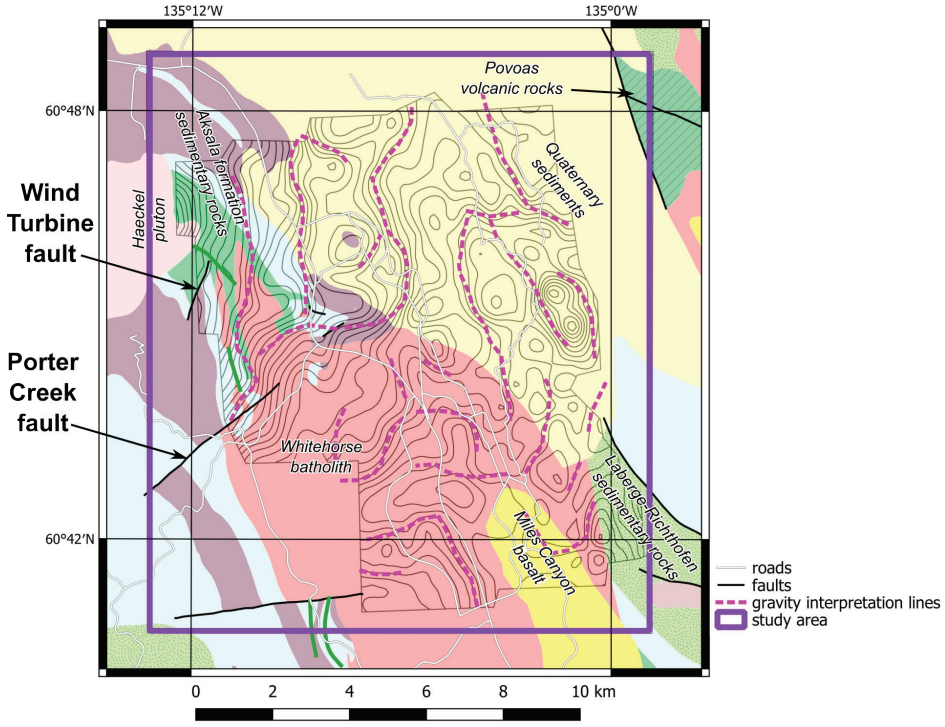

Figure 12. *Bedrock geology map of the study area with CBA gravity contours (thin black lines) and gravity interpretation lines (pink dashed lines) overlain. Major rock units and faults are labelled. Bedrock map legend shown in Figure 3. See text for discussion.*

Magnetic survey data

Within the study area, the Total Magnetic Intensity (TMI) map with Reduction to Pole (RTP) applied has the range -375 nT to +650 nT (Fig. 13). Overall, the Total Magnetic Intensity – Reduced to Pole (TMI-RTP) data generally correspond to the mapped geology (Fig. 14). Key features of the magnetic map include:

- A strong magnetic high on the NW side of the study area that coincides with the Haeckel Hill pluton.
- Strong magnetic high anomalies associated with the northern half of the Whitehorse batholith.
- More moderate magnetic response for the southern half of the Whitehorse batholith.
- The sedimentary rocks of the Aksala formation (i.e., Mandanna, Hancock and Casca) lie on the flank of the granitic rocks in a region of rapidly decreasing magnetic intensity.
- The Miles Canyon basalt is characterized by a variable magnetic response.
- The area covered by Quaternary sediments is dominated by low magnetism.
- Both the Wind Turbine fault and the Porter Creek fault lie along the southern edges of strong magnetic high anomalies suggesting these anomalies may be fault-controlled.

Hand samples of the Haeckel Hill pluton yield moderately high values for magnetic susceptibility and may be the geologic explanation for the strong magnetic response observed

on the NW side of the study area. However, the strong magnetic response may also be influenced by contact metamorphism and mineralization which could crystallize significant amounts of magnetite. This explanation is consistent with the high gravity anomaly observed in the same location.

Similar to the gravity map, a THG filter was applied to the TMI-RTP data to highlight the zones of greatest horizontal change in the magnetic data (Fig. 13). In this case, the total horizontal gradient can be used to infer faults or rock unit contacts that separate rocks with differing magnetism. Based upon comparison with the bedrock geology, many of the interpretation lines inferred from the TMI-RTP map appear to represent the edges of the igneous rock bodies (Fig. 14). However, the reason for the stronger magnetic response for the northern half of the Whitehorse batholith (compared to the southern half) remains unexplained.

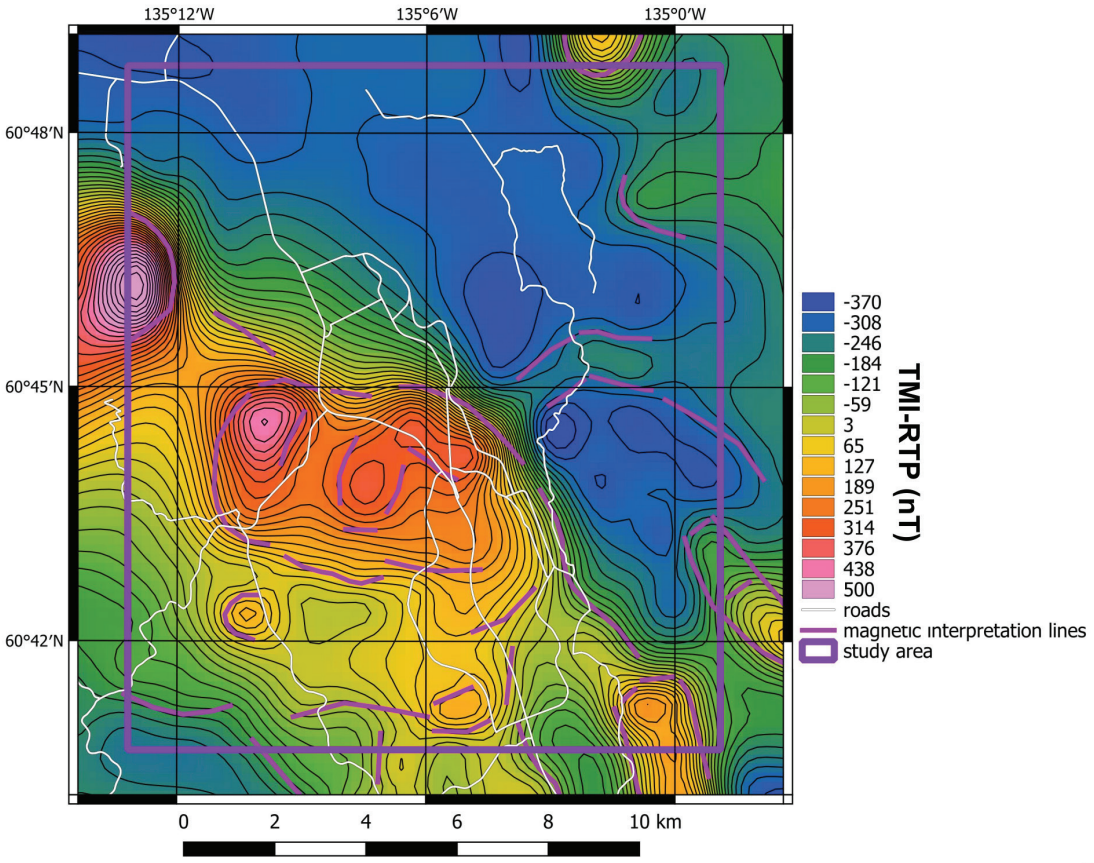

Figure 13. *Public domain, regional-scale magnetic survey data plotted as Total Magnetic Intensity – Reduced to Pole (TMI-RTP) and gridded with a 200 m cell size. Magnetic contours (thin black solid lines) are shown at 25 nT intervals. Cool/warm colours represent magnetic lows/highs. Interpretation lines (pink solid lines) were inferred from another magnetic map (not shown) with a Total Horizontal Gradient filter applied (Appendix B). The study area is indicated by the purple rectangle.*

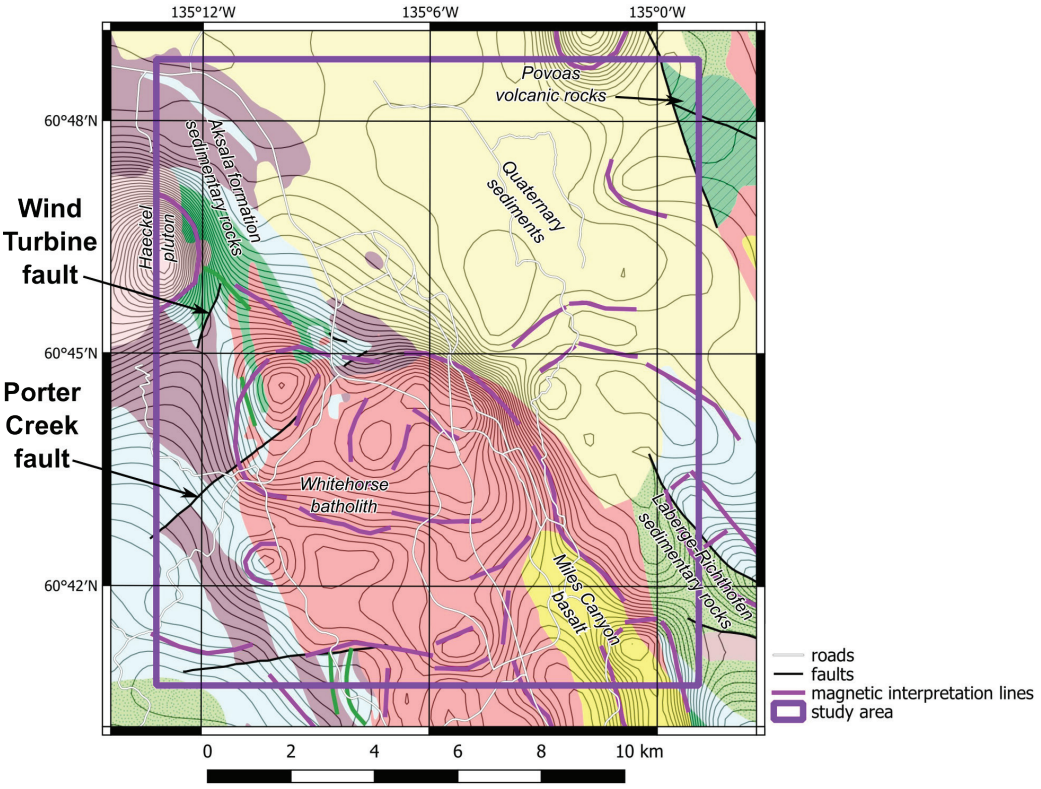

Figure 14. *Bedrock geology map of the study area with TMI-RTP magnetic contours (thin black lines) and magnetic interpretation lines (pink solid lines) overlain. Major rock units and faults are labelled. Bedrock map legend shown in Figure 3. See text for discussion.*

A comparison of the regional magnetic survey data and the high-resolution data is shown in Figure 15. The spatial resolution of the high-resolution data is approximately 50 times better than the regional magnetic data. The two magnetic datasets are similar in that the regional magnetic data broadly characterizes many of the same high and low magnetic anomalies that are seen in the high-resolution magnetic data that are associated with the different rock units. However, the high-resolution data capture an enormous amount of detail that is simply missing in the regional dataset.

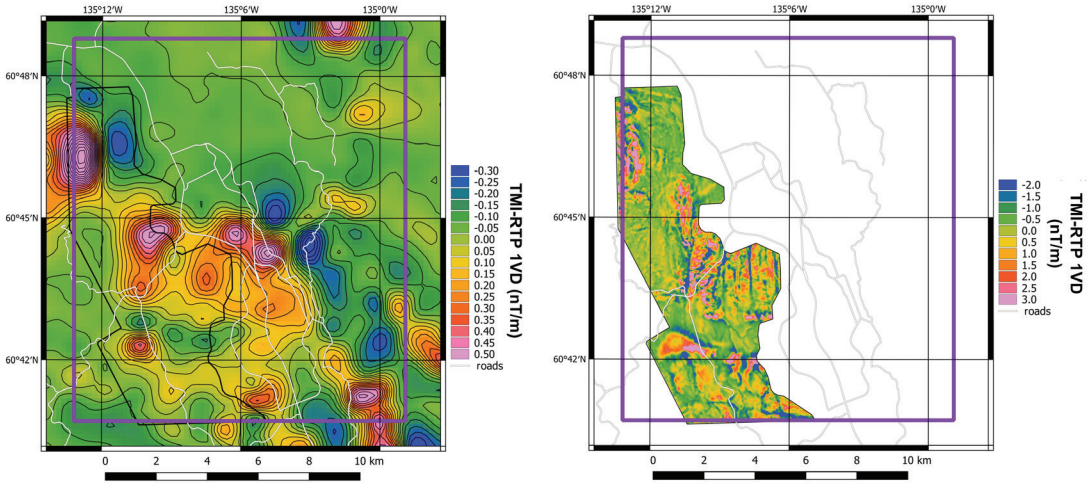

Figure 15. *TMI-RTP maps with 1st vertical derivative (1VD) filter applied that compare the regional magnetic survey data (left panel) with the high-resolution magnetic survey data provided by Gladiator Metals Corp (right panel).*

Integrated 3D geoscience model interpretation

2D gravity profile modelling

Eight, simple 2D gravity profile models were constructed across the gravity survey area (Fig. 16). The purpose of these profile models is to provide rough estimates of the thickness of glacial sediments along each profile. However, one of the drawbacks of this exercise is that each 2D profile was constructed independently of one another. This created a mismatch where the profiles cross. In addition, for the 2D profiles, Casca and Povoas rocks were merged into a single unit to simplify the modelling. For these reasons, the results of the 2D profile modelling were only used as a rough starting point for the top-of-bedrock surface. Overall, the 2D profile models suggest that the thickness of glacial sediments varies between 0 and ~500 m. Two example profiles are shown in Figure 17 (all profiles are in Appendix B). A rough, 3D top-of-bedrock surface was constructed by interpolating between the 2D profiles, while at the same time honouring: a) known areas where bedrock is exposed at the surface (i.e., depth-to-bedrock ≈ 0 m); and b) depth-to-bedrock data from water wells. This surface was then further refined in the 3D geology + gravity + magnetic modelling described below.

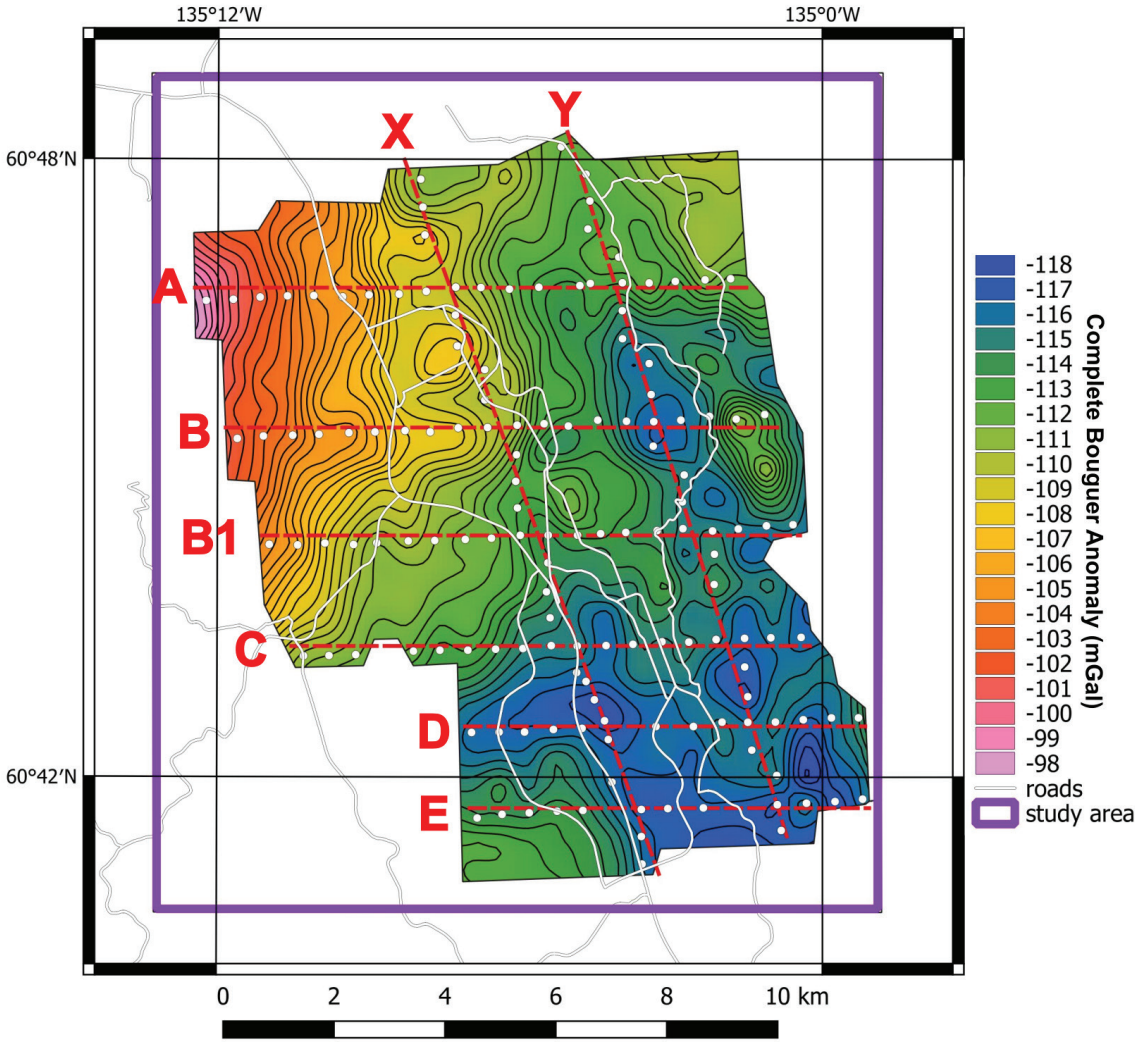

Figure 16. *Complete Bouguer Anomaly gravity map showing the locations of the simple 2D gravity profile models (red dashed lines with labels) and the gravity data points used to construct each profile (white dots).*

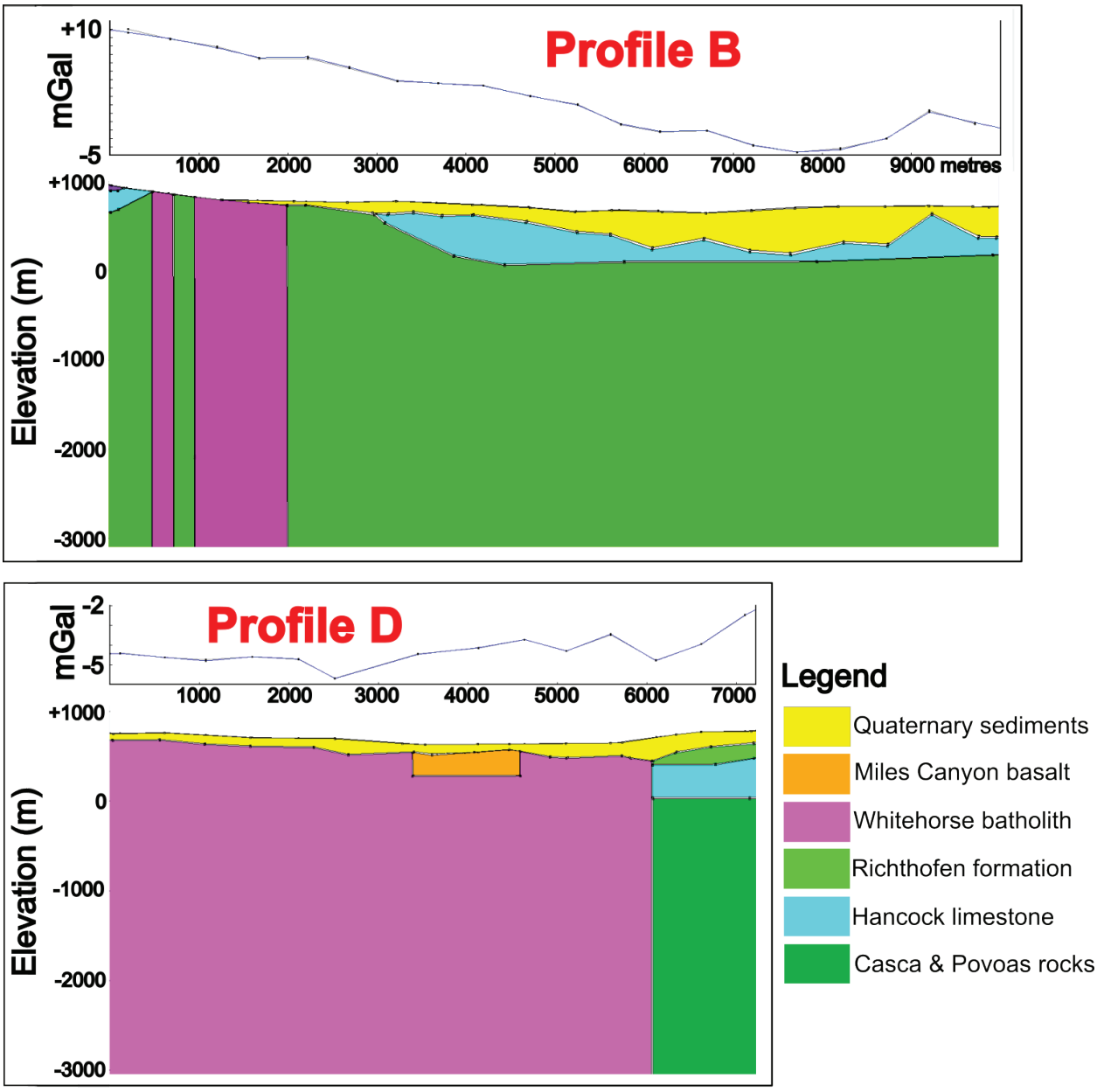

Figure 17. *2D gravity profile model B (top panel) and D (bottom panel). Bedrock units are shown in the legend. In each panel, the lower diagram is the modelled 2D geologic cross-section consisting of different rock units and the graph above it shows the observed and calculated gravity data (in mGal) along the profile. The gravity profile vs. distance graphs appear as a single line because the observed and calculated data fall on top of one another.*

3D geology + gravity + magnetic modelling

A 3D geologic model was constructed to provide a framework to help better interpret regions of potential geothermal favourability in the Whitehorse area (Fig. 18). A key goal of the 3D geologic model building exercise is to build a geologic volume consisting of fault planes, folds and discrete blocks of rock that are, as much as possible, consistent with all the available geoscience data. Information used to construct the initial 3D geologic model includes:

- Bedrock geology map;
- Regional stratigraphy;

- Mapped geologic structures such as folds and faults;
- Areas of near zero sediment cover based on surficial geology data;
- Depth-to-bedrock information from water wells;
- Sediment thickness estimates from 2D gravity profiles.

When constructing the stratigraphy in the 3D geologic model the thickness of the Miles Canyon basalt unit was assumed to be 300 to 400 m (Wheeler, 1961; Hart and Radloff, 1990). The maximum thicknesses of Lewes River Group rocks were assumed to be the following: Mandanna – 1 km; Hancock – 600 m; Casca – 1 km; and Povoas – 2 km (Hart, 1997b).

Once the 3D initial geologic framework for the bedrock was constructed, 3D gravity and magnetic inversion modelling were performed separately to test and refine the initial 3D geology framework. Specifically, the 3D gravity inversion modelling was run multiple times to refine the top-of-bedrock surface. In addition, 3D magnetic vector inversion modelling was run to test whether reversely magnetized rock bodies (e.g., Miles Canyon basalt and Povoas formation) would better fit the measured magnetic survey data.

For each 3D gravity inversion, different rock units in the 3D geologic model were assigned reference density values based upon rock density measurements (Table 1). Similarly, for each 3D magnetic inversion, the rock units in the 3D geologic model were assigned reference magnetic susceptibility, declination and inclination values. In the inversion calculations, the inversion algorithm adjusted the rock property values (density, magnetic susceptibility, declination and inclination) in the model cells until a match was achieved with the measured geophysical data. For the gravity modelling, a match was achieved when the root-mean-squared (RMS) misfit, calculated for the 3D density model, reached a nominal value of 0.1 mGal (slightly higher than the average measurement error of the gravity survey data of 0.05 mGal). The actual calculated RMS misfit obtained for the final 3D density model is 0.13 mGal. Similarly, the estimated error on the magnetic survey data is ~5 nT; we used this value as the target misfit during the magnetic inversion modelling. The 3D magnetic vector inversion model that was generated during the inversion modelling achieved an actual RMS misfit of 4.1 nT. Thus, both the gravity and magnetic inversion modelling exercises reached the target misfit values and the model outputs are considered consistent with the geophysical survey data.

The final 3D geologic model (Fig. 18) contains nine different rock units (Table 2) and largely honours the bedrock and surficial geology mapping of the Yukon Geological Survey (2023b) and Lipovsky (2023).

Table 2. *List of rock units in the Whitehorse 3D geologic model. * = rock unit is part of the Aksala formation. 1 = for the 3D magnetic inversion modelling, the Mandanna unit was divided into two subunits: Mandanna West (more magnetic) and Mandanna North (less magnetic).*

Rock unit name	Age	Rock type
Quaternary sediments	Quaternary	Glacial sediments
Miles Canyon basalt	Miocene	Basalt
Haeckel Hill pluton	Eocene	Granite
Whitehorse batholith	mid-Cretaceous	Granodiorite and quartz diorite
Richthofen formation	Jurassic	Shale/sandstone/conglomerate
Mandanna member*[1]	Upper Triassic	Greywacke/conglomerate/mudstone
Hancock member*	Upper Triassic	limestone
Casca member*	Upper Triassic	Shale/siltstone/greywacke/limestone
Povoas formation	Upper Triassic	Andesitic basalt/sandstone/argillite

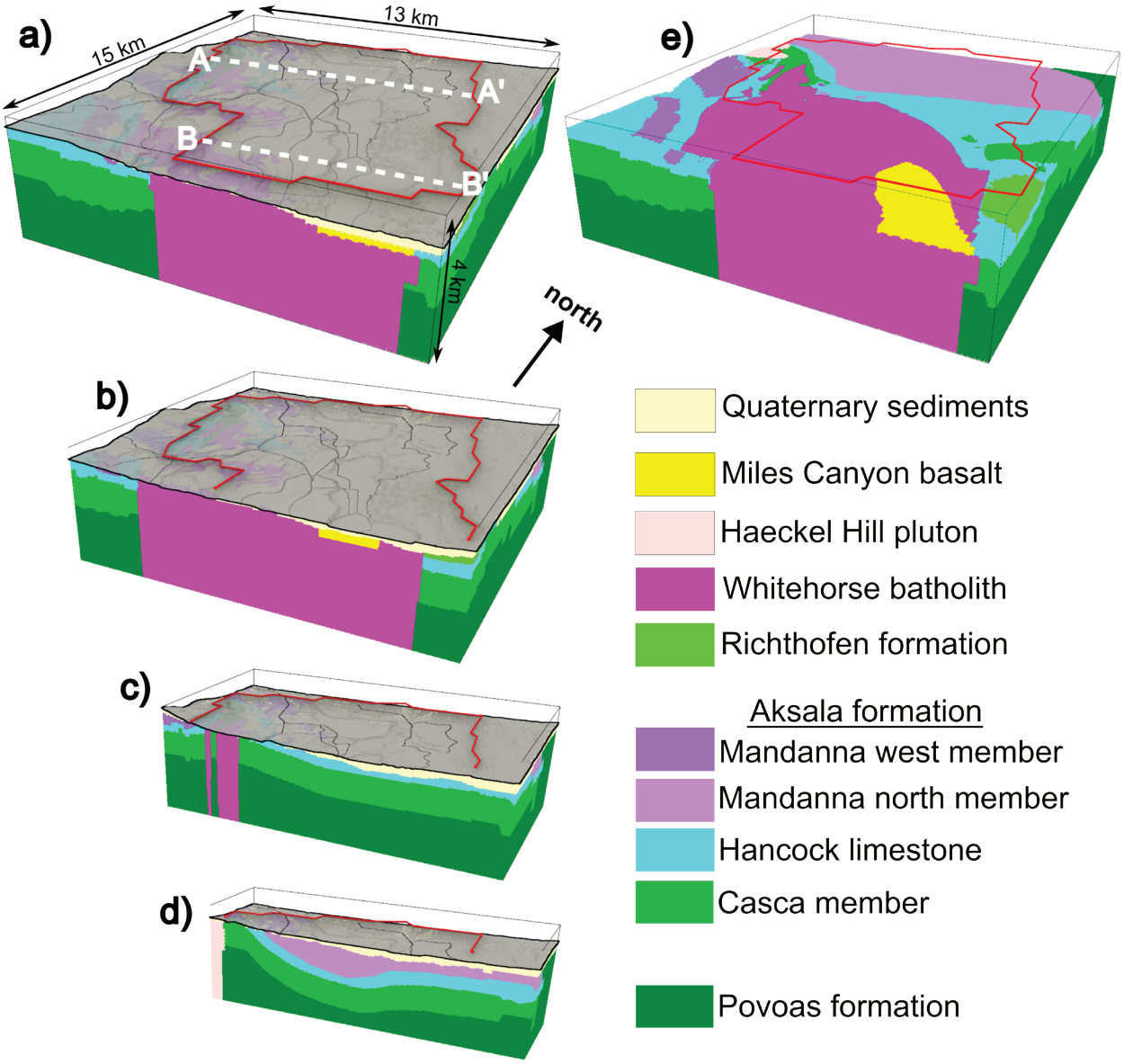

Figure 18. *Perspective view of the 3D geology model for the Whitehorse area.* ***a)*** *Entire 3D geology model that shows all rock units covered by topography (translucent grey) with roads overlain (black lines). Red polygon defines the extent of the gravity survey—outside of the red polygon the 3D geology model is of lower quality because it has not been constrained by gravity data.* ***b), c)*** *and* ***d)*** *show various E-W slices through the 3D geology model.* ***e)*** *Entire 3D geology model with topography and glacial sediments removed. Dashed white lines in (a) show the locations of 2D cross-sections A-A' and B-B' extracted from the 3D model shown in Figures 19–26.*

Many assumptions went into the creation of the 3D geologic model. For example, it is assumed that the density and magnetic susceptibility of the Quaternary sediment are, on average, 2.0 g/cm^3 and 0 SI, respectively. The density value is likely not correct since it would be expected glacial lake sediments and glacial till (which are lumped together here) to have different densities. However, in the absence of rock density measurements for the Quaternary sediments, the 2.0 g/cm^3 estimate suffices for the geophysical modelling performed here. It is also assumed that other rock units have a generally uniform density and magnetic susceptibility (i.e., no significant variations laterally or vertically within a single rock

unit). Faults are assumed to be steeply dipping or vertical. Similarly, due to an absence of information, the intrusive contacts for the Haeckel Hill pluton and Whitehorse batholith are assumed to be vertical. Furthermore, the thicknesses of stratigraphic units in the 3D geologic model are assumed to be laterally continuous since it is not known how much these units thicken or thin with distance. Due to these many assumptions and the uncertainty associated with them, the 3D geologic model is not intended to be a 100% accurate depiction of the subsurface; rather, it is meant to be as close to reality as possible, to be improved in the future with additional geophysical data and/or drilling results.

The overall outcome of the 3D geology + gravity + magnetic inversion modelling effort includes new 3D rock density and 3D magnetic models with faulted and stratigraphic geologic boundaries. Two cross sections have been extracted from the 3D rock property models that run along E-W profiles (Figs. 19–26). Although the rock property models are in three dimensions, the 2D cross sections presented here highlight some of the key elements of the rock property models.

The 2D cross sections showing density model results (Figs. 19 and 23) contain the following elements: a reference geologic model (showing rock types and reference density values used for the geologic constraints), and a geologically constrained density inversion model output (the best attempt made to reconcile geology, gravity data and rock property measurements). The density model results are presented using a 2.5 to 2.9 g/cm^3 colour scale to visualize the variation of density in the models.

The 2D cross sections that show magnetic vector inversion results (Figs. 20–22 and 24–26) contain similar elements and come in three parts: susceptibility, declination, and inclination. Together, these three parts define the rock's magnetic susceptibility and the direction (declination and inclination) of the magnetization. The susceptibility model results are visualized using a log colour scale with the range 0.0001 to 0.05 SI units. The declination model results (Figs. 21 and 25) use a linear colour scale from 0° to 360° and the inclination model results (Figs. 22 and 26) use a linear colour scale from -90° to +90°.

By comparing the various model results with their reference geology and rock property models we can gain insight into how good the match is between our conceptual understanding of the subsurface geology and reality. In some areas, the agreement between the reference and inversion rock property models is good. In other areas, regions of mismatch are clear and represent areas where the geologic understanding is reduced and more information is needed to help better understand the subsurface.

Explanation of cross section A-A': through Versluce warm spring

The E-W cross section through Versluce warm spring contains six of the nine rock units found in the study area (Fig. 19). Key features of the geology model in this section include: a layer of Quaternary sediments that is thicker on the east side of the profile; bedrock is at or very near the surface on the west side; intrusions (of uncertain shape) of granitic Whitehorse batholith rocks are found on the west side; and rocks of the Aksala formation have been folded and form an anticline on the west side of the section. Note that the Haeckel Hill pluton lies just off section, immediately NW of the west end of cross section A-A'.

The geologically constrained density inversion model result for cross section A-A' shows mostly a good match between the reference model and inversion results (Fig. 19a,b) except for the following points described here. A small and localized density mismatch can be seen in the centre of the section, just below the Quaternary sediments (Fig. 19b, point #1) and this is likely due to excessively thick Quaternary sediments in the reference model at this location. Reducing

the thickness of Quaternary sediments at point #1 by 40 to 80 m (1–2 model cells) would likely fix this mismatch. The deepest portion of the Povoas formation (Fig. 19b, point #2) does not match the reference density model across a wide area. The inversion model result suggests that lower density rocks (~2.75 g/cm^3) rocks are needed, not the higher density (~2.88 g/cm^3) value assigned to the Povoas formation. This can be interpreted as either: a) the high rock density values for the Povoas formation measured in hand samples are not representative of this unit in this area; or b) the Povoas formation in the reference geology model is too thick and the Povoas formation is underlain by a different, lower density rock unit. Lastly, there is a clear density mismatch between the reference model and inversion results beneath the Versluce warm spring (Fig. 19b, point #3). In order to match the gravity data, the inversion results suggest that lower density rocks are needed, vertically, through the entire stratigraphic section with the strongest density mismatch occurring in the Povoas unit. Specifically, the reference density of the Povoas unit is 2.88 g/cm^3 and the inversion result suggests rock density as low as ~2.60 g/cm^3 might be more appropriate. Coincidentally, the measured density value for Haeckel Hill pluton rocks is ~2.60 g/cm^3. Thus, a simple explanation of this density mismatch could be that lower density Haeckel Hill pluton rocks intruded into the Povoas and Casca units (and possibly even shallower?) at a location beneath the Versluce warm spring.

The geologically constrained magnetic vector inversion model results for cross section A-A' (Figs. 20–22) show only fair agreement with the reference models. For this modelling effort, we assumed that the Povoas formation has the highest magnetic susceptibility and is reversely magnetized while all other rock units have lower magnetic susceptibility values and are normally magnetized. There is generally poor agreement between the reference model and inversion results in the uppermost 2 km of the profile for the rock units with low magnetic susceptibility (Fig. 20b, point #1). This is not surprising since it is difficult for the inversion algorithm to accurately model the variation at such low levels of susceptibility (e.g., 10^{-3}–10^{-4} SI). One other area of mismatch is the Whitehorse batholith intrusions on the west side of the section (Fig. 20b,c, point #2). Curiously, the inversion model result using the regional-scale magnetic survey data (Fig. 20b) shows the upper portions of the Whitehorse batholith has lower magnetic susceptibility than the lower portion. In contrast, the inversion model using the high-resolution magnetic survey data (Fig. 20c) shows nearly all the Whitehorse batholith intrusive rocks have similar, elevated magnetic susceptibility. The inversion model using the high-resolution survey data is more accurate since it is informed by a high density of magnetic survey datapoints, whereas there are no regional-scale magnetic survey datapoints above point #2 because it falls between the 1.5 km spaced regional survey lines. Despite this improvement using the high-resolution magnetic survey data, the magnetic susceptibility value for the Whitehorse batholith returned by the inversion model is about an order of magnitude higher than the reference model value for these rocks (0.05 SI vs. 0.006 SI); this remains unexplained. Lastly, the inversion model result suggests that higher magnetic susceptibility values are needed in the Casca member rocks across a broad area beneath the Versluce warm spring to agree with the magnetic survey data (Fig. 20b, point #3). One way to explain this mismatch would be the presence of higher susceptibility granitic rocks that have intruded into the lower susceptibility Casca rocks. This hypothesis is broadly consistent with the results of the gravity inversion; however, the magnetic susceptibility inversion model does a poor job of defining the geometry of the intruded rocks. What also remains unexplained is why the magnetic inversion model requires magnetic susceptibility values in the Povoas formation that are about an order of magnitude higher than the reference model value.

The declination and inclination model results (Figs. 21 and 22) suggest that parts of the Povoas formation are likely reversely magnetized, in agreement with the magnetic polarity

timescale. However, the inversion result using the regional-scale magnetic survey data (Figs. 21b and 22b) does a much poorer job of resolving the reversely magnetized Povoas rocks compared to the inversion that used the high-resolution magnetic data (Figs. 21c and 22c).

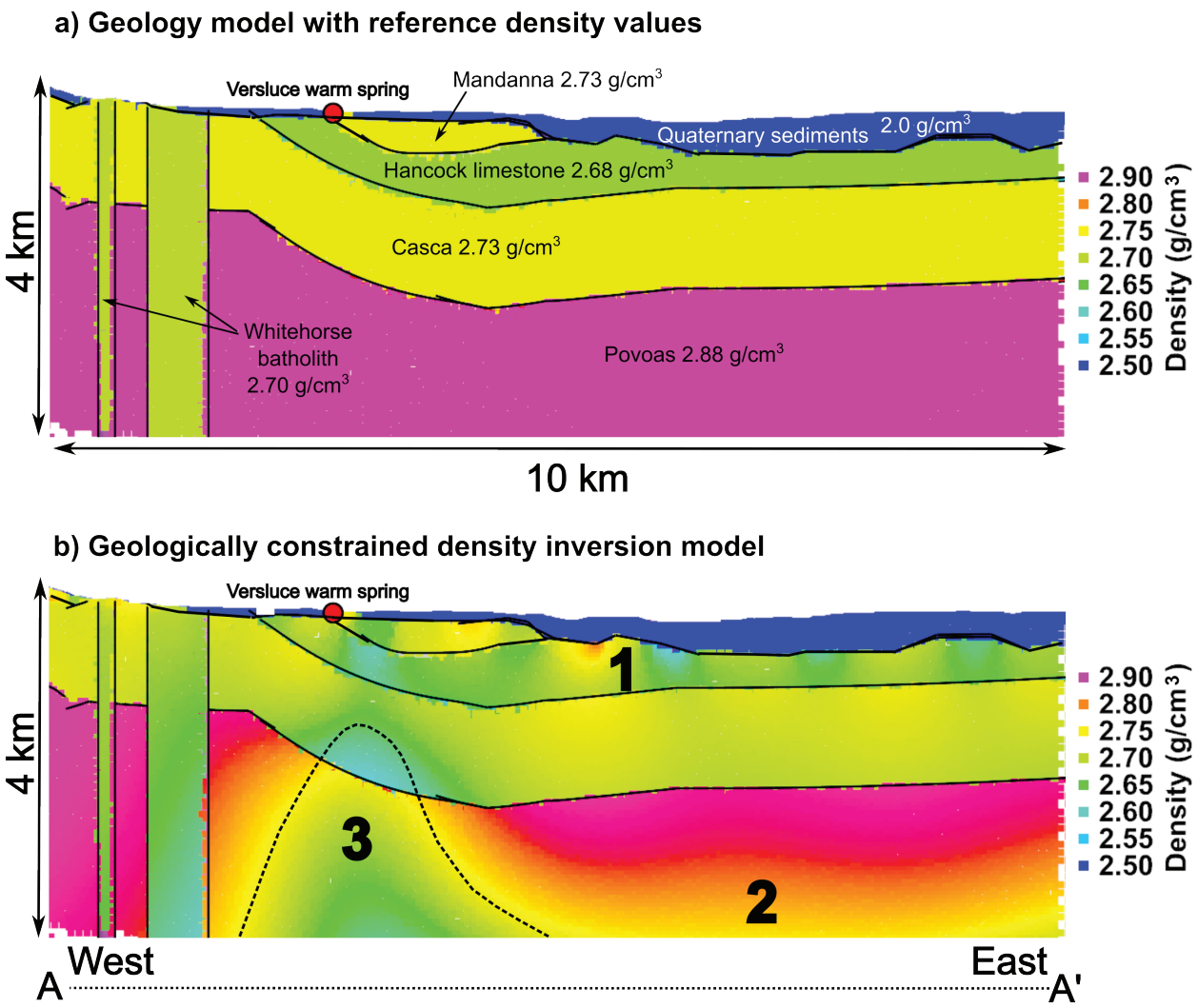

Figure 19. *Density model cross-sections along A-A' through Versluce warm spring.* ***a)*** *Geology model with reference rock density values used to constrain the 3D gravity modelling.* ***b)*** *Rock density distribution returned by the 3D gravity inversion modelling that honours the gravity data. The match between the reference rock density model (a) and the inverted rock density model (b) is fairly good except for the three locations labelled 1, 2 and 3. Black dashed line shows approximate extent of low density rocks (Haeckel Hill pluton?) needed to agree with the observed gravity data. See text for further explanation.*

Explanation of cross section B-B': through the Miles Canyon basalt aquifer

The E-W cross section B-B' was selected to pass through the southern portion of the study area and the TH02-01 well at the St. Francis of Assisi Catholic Secondary School. This well encountered the Selkirk aquifer in shallow sediments as well as the deeper Miles Canyon basalt aquifer.

This cross section contains seven of the nine rock units found in the study area (Fig. 23a). Key

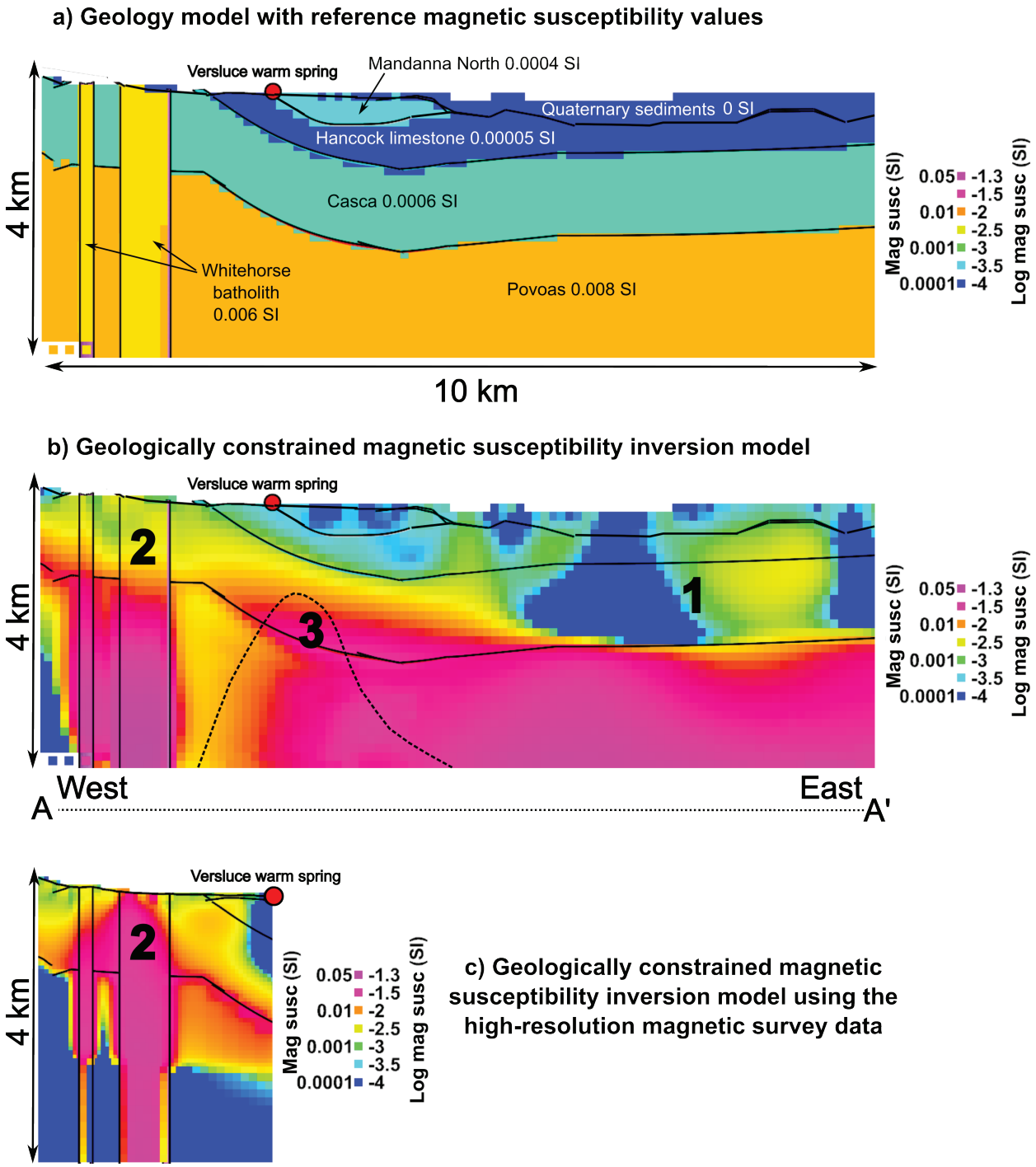

Figure 20. *Magnetic susceptibility model cross-sections along A-A' through Versluce warm spring.* ***a)*** *Geology model with reference rock magnetic susceptibility values used to constrain the MVI modelling.* ***b)*** *Magnetic susceptibility distribution returned by the 3D MVI inversion modelling that honours the regional-scale magnetic survey data.* ***c)*** *Magnetic susceptibility distribution returned by the 3D MVI inversion modelling that honours the high-resolution magnetic survey data. The match between the reference susceptibility model (a) and the inverted susceptibility models (b and c) is fair but it is particularly poor in three locations labelled 1, 2 and 3. Black dashed line marks the low-density anomaly from Figure 19. See text for further explanation. A log scale is used for the magnetic susceptibility values to help better visualize the results.*

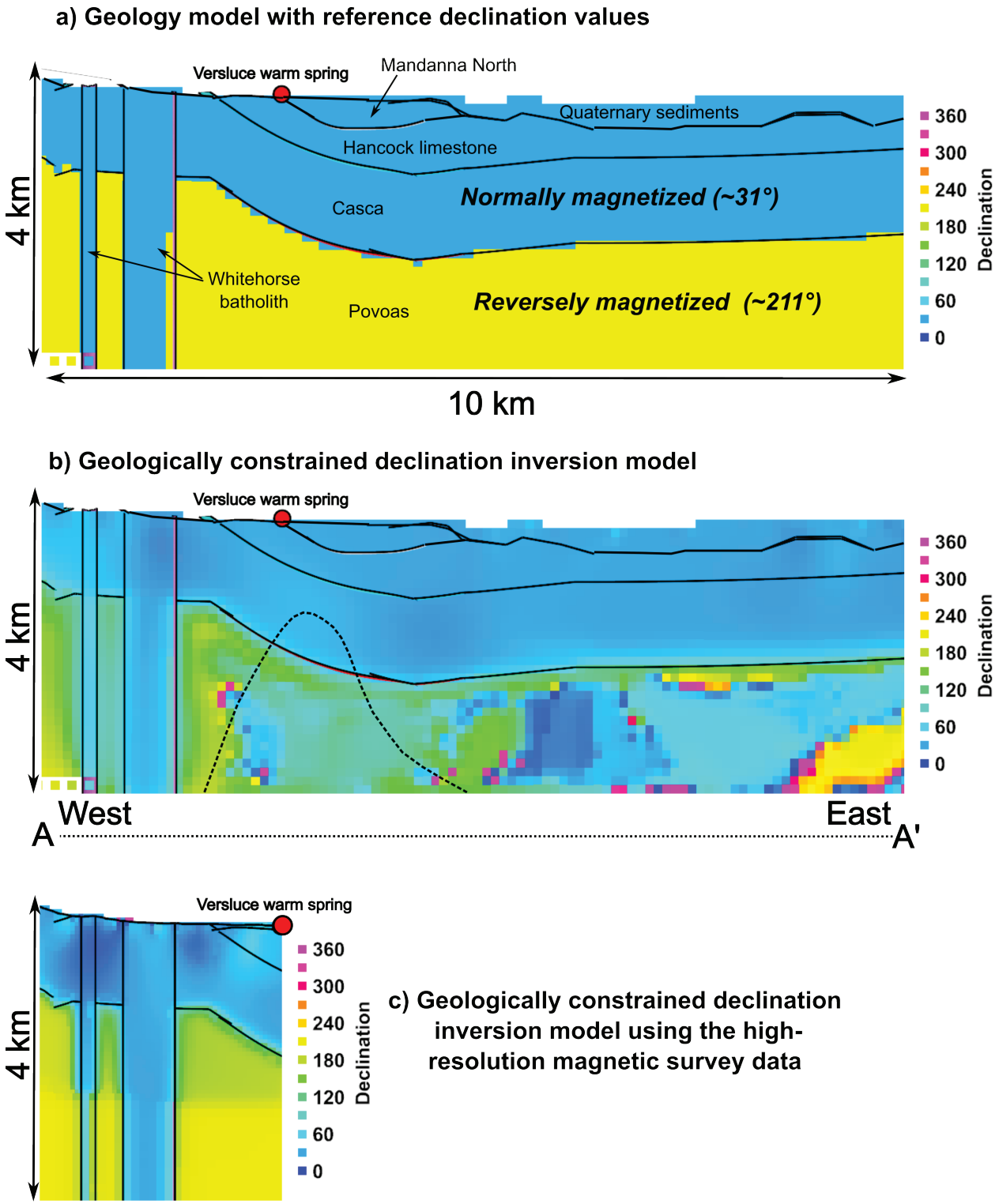

Figure 21. *Declination model cross-sections along A-A' through Versluce warm spring.* ***a)*** *Geology model with reference declination values used to constrain the MVI modelling.* ***b)*** *Declination distribution returned by the 3D MVI inversion modelling that honours the regional-scale magnetic survey data.* ***c)*** *Declination distribution returned by the 3D MVI inversion modelling that honours the high-resolution magnetic survey data. The match between the reference declination (a) and the inverted declination models (b and c) is fair but it is particularly poor for the Povoas formation shown in (b). Black dashed line marks the low-density anomaly from Figure 19. See text for further explanation.*

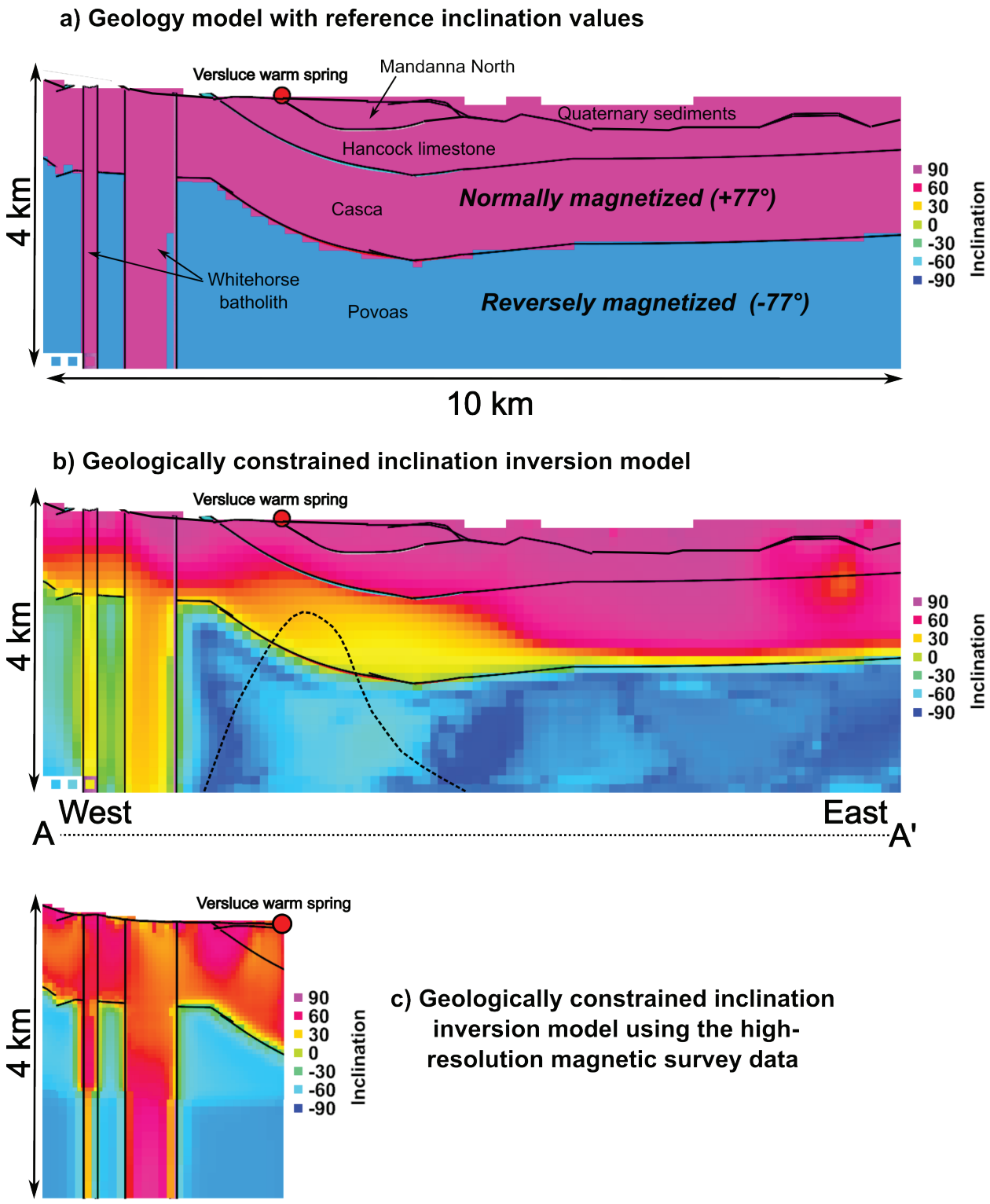

Figure 22. *Inclination model cross-sections along A-A' through Versluce warm spring.* **a)** *Geology model with reference inclination values used to constrain the MVI modelling.* **b)** *Inclination distribution returned by the 3D MVI inversion modelling that honours the regional-scale magnetic survey data.* **c)** *Inclination distribution returned by the 3D MVI inversion modelling that honours the high-resolution magnetic survey data. The match between the reference inclination (a) and the inverted inclination models (b and c) is fair but it is particularly poor for portions of the Casca and Povoas rock units shown in (b). Black dashed line marks the low-density anomaly from Figure 19. See text for further explanation.*

features of the geology model in this area include: a layer of Quaternary sediments that is thicker on the east side of the profile; a large body of granitic Whitehorse batholith rocks with an (assumed) vertical contact on its eastern edge; typical Mesozoic stratigraphy lie adjacent to the Whitehorse batholith; and a relatively thin section of Miles Canyon basalt rocks assumed to be a few hundred metres thick. In this profile, the thickness of the Quaternary sediments and Miles Canyon basalt are constrained by the TH02-01 well.

The geologically constrained density inversion model for cross section B-B' shows a fair match between the reference model and inversion results (Fig. 23a,b). For most of the Whitehorse batholith and Mesozoic stratigraphy, the inversion model generally agrees with the density values in the reference model. However, the match is poor at four locations (Fig. 23b, points #1–4). At point #1, there is a poor match immediately beneath the TH02-01 well, which suggests that the reference density value for the Miles Canyon basalt may be inaccurate (i.e., the Miles Canyon basalt may have a lower density than assumed). At point #2, the inversion result needs lower density rocks compared to the reference model. This mismatch would likely be remedied by a minor increase (tens of metres) in the thickness of the overlying Quaternary sediments. According to the inversion model result, lower density rocks are needed in the lower half of the Povoas unit (point #3). This outcome is similar to the density model in section A-A' and could be explained by a lower density rock unit present beneath the Povoas formation. The inversion model result at point #4 shows a much lower density value (~2.50 g/cm^3) compared to the reference value (2.75 g/cm^3) for Whitehorse batholith rocks. This result is difficult to explain as it is unclear whether this is an artefact of the modelling or a reflection of the geology.

The geologically constrained magnetic vector inversion model results for section B-B' (Figs. 24–26) show a fair match between the reference and inversion model results. The Quaternary sediments, Miles Canyon basalt, and much of the Whitehorse batholith, show general agreement with the reference magnetic susceptibility, declination and inclination models. However, significant mismatch exists near the eastern margin of the Whitehorse batholith (point #1). The inversion model results suggest a strongly magnetic and potentially reversely magnetized rock unit exists at ~2 km depth on the east side of the cross section. The exact geometry of this rock unit is poorly characterized by the magnetic inversion modelling. This observed mismatch likely arises because: a) the contact for the Whitehorse batholith has been assumed to be vertical (as shown in the reference model) when it may actually have a very different geometry; b) a reversely-magnetized portion of the Povoas formation may extend further west than shown in the reference model; or c) another plutonic body (different from the Whitehorse batholith and with different magnetic properties) may have intruded into this area. Another observation of the magnetic susceptibility model result along B-B' is that the magnetic inversion model requires magnetic susceptibility values in the Povoas formation that are about an order of magnitude higher than the reference model value (point #2). This is similar to what is observed in section A-A' and suggests that these rocks may be more magnetic than the measured Povoas rock samples. Lastly, unusually low magnetic susceptibility values appear in the model result in the bottom-central portion of profile B-B' (point #3). One possibility is that this could represent the base of the Whitehorse batholith in this area.

Overall, this 3D geophysical modelling exercise has: helped to confirm large portions of the 3D geologic model; identified areas where the 3D geologic model is inaccurate; and generated a new depth-to-bedrock estimate for the Whitehorse study area.

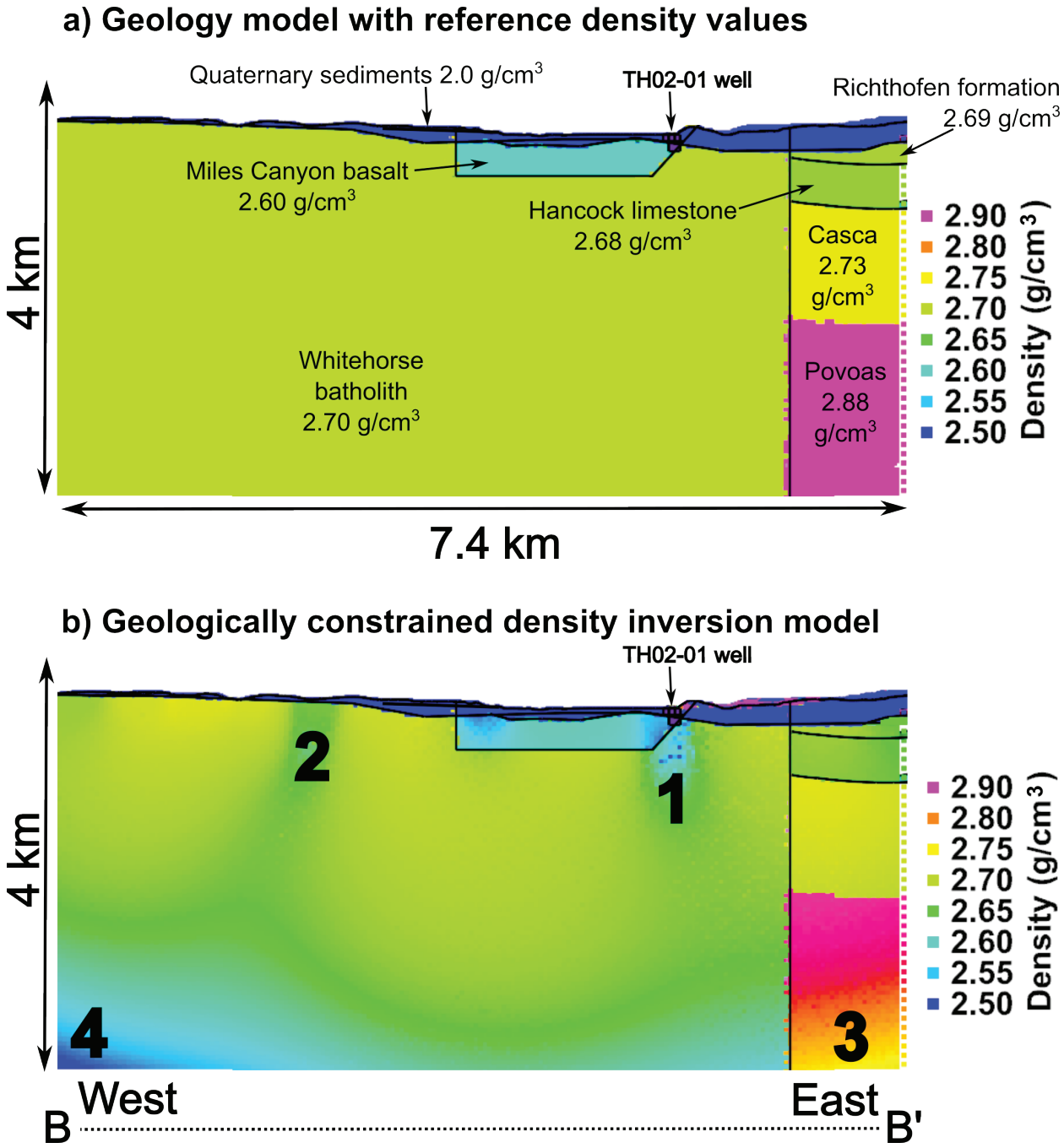

Figure 23. *Density model cross-sections along B-B' through the Miles Canyon basalt.* ***a)*** *Geology model with reference rock density values used to constrain the 3D gravity modelling.* ***b)*** *Rock density distribution returned by the 3D gravity inversion modelling that honours the gravity data. The match between the reference rock density model (a) and the inverted rock density model (b) is fairly good except for the four locations labelled 1, 2, 3 and 4. See text for further explanation.*

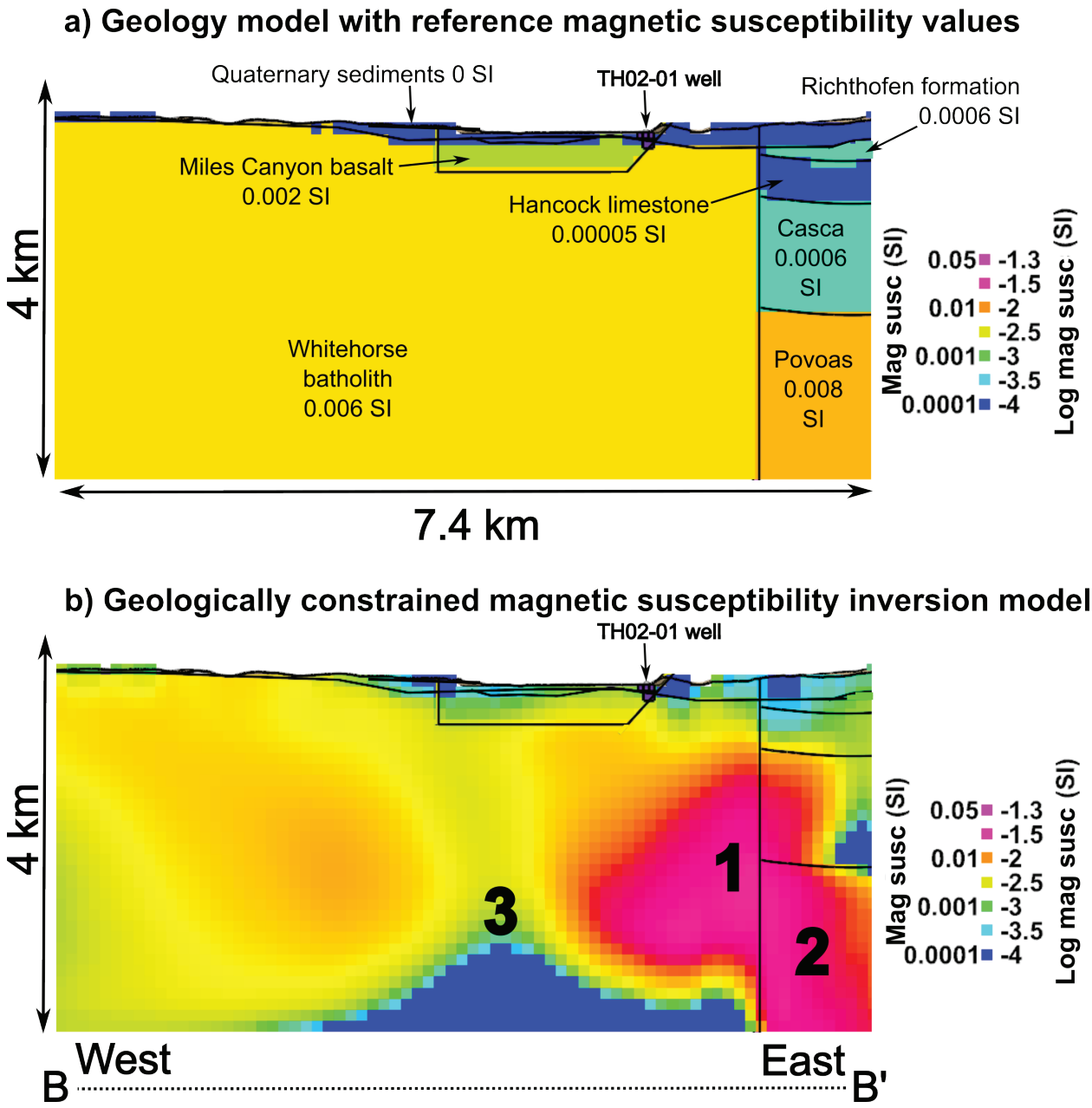

Figure 24. *Magnetic susceptibility model cross-sections along B-B' through the Miles Canyon basalt.* ***a)*** *Geology model with reference rock magnetic susceptibility values used to constrain the MVI modelling.* ***b)*** *Magnetic susceptibility distribution returned by the 3D MVI inversion modelling that honours the regional-scale magnetic survey data. The match between the reference susceptibility model (a) and the inverted susceptibility model (b) is fair but it is particularly poor in three locations labelled 1, 2 and 3. See text for further explanation. A log scale is used for the magnetic susceptibility values to help better visualize the results.*

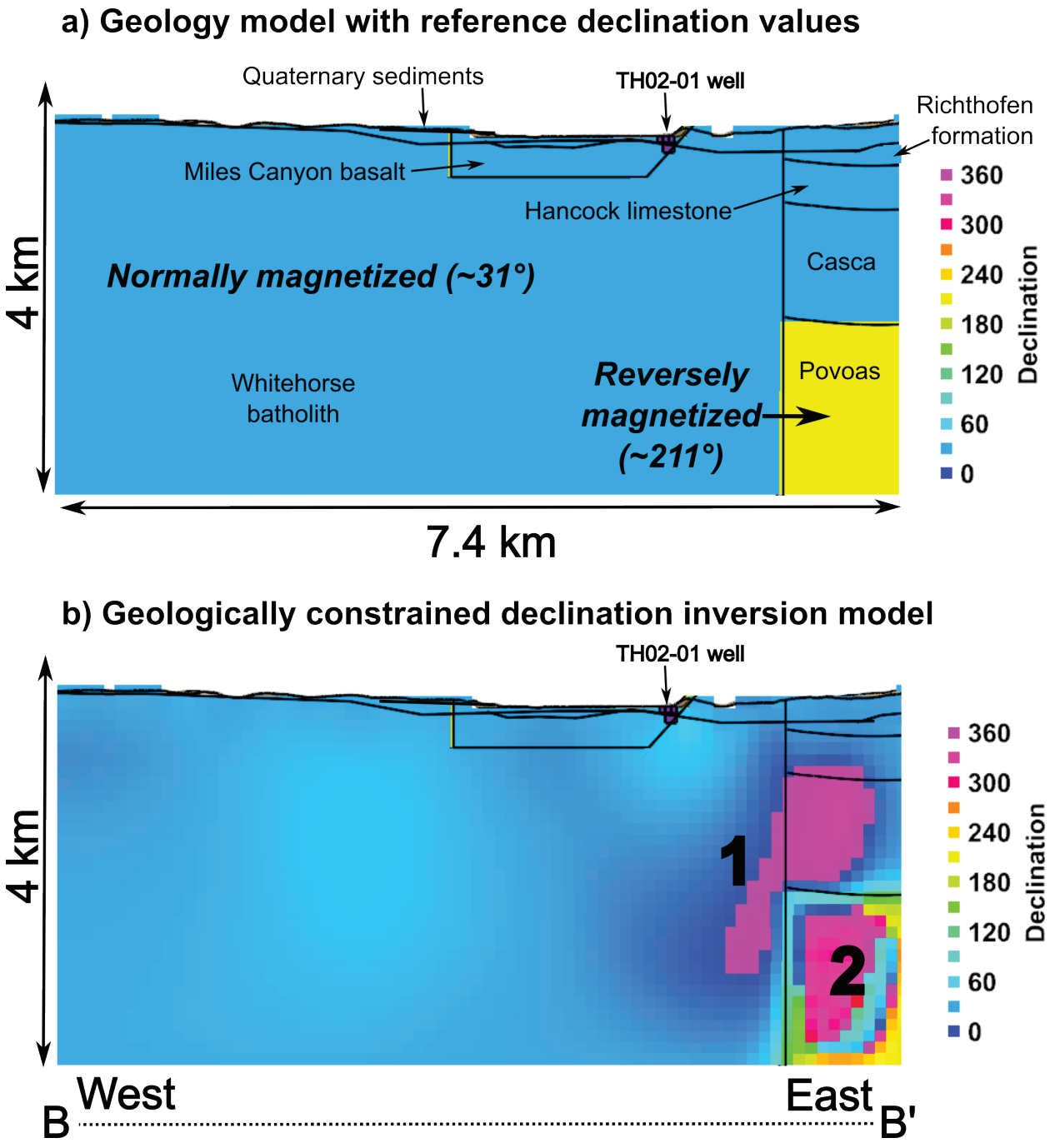

Figure 25. *Declination model cross-sections along B-B' through the Miles Canyon basalt.* ***a)*** *Geology model with reference declination values used to constrain the MVI modelling.* ***b)*** *Declination distribution returned by the 3D MVI inversion modelling that honours the regional-scale magnetic survey data. The match between the reference declination (a) and the inverted declination model (b) is fair but it is particularly poor in the locations labelled 1 and 2. See text for further explanation.*

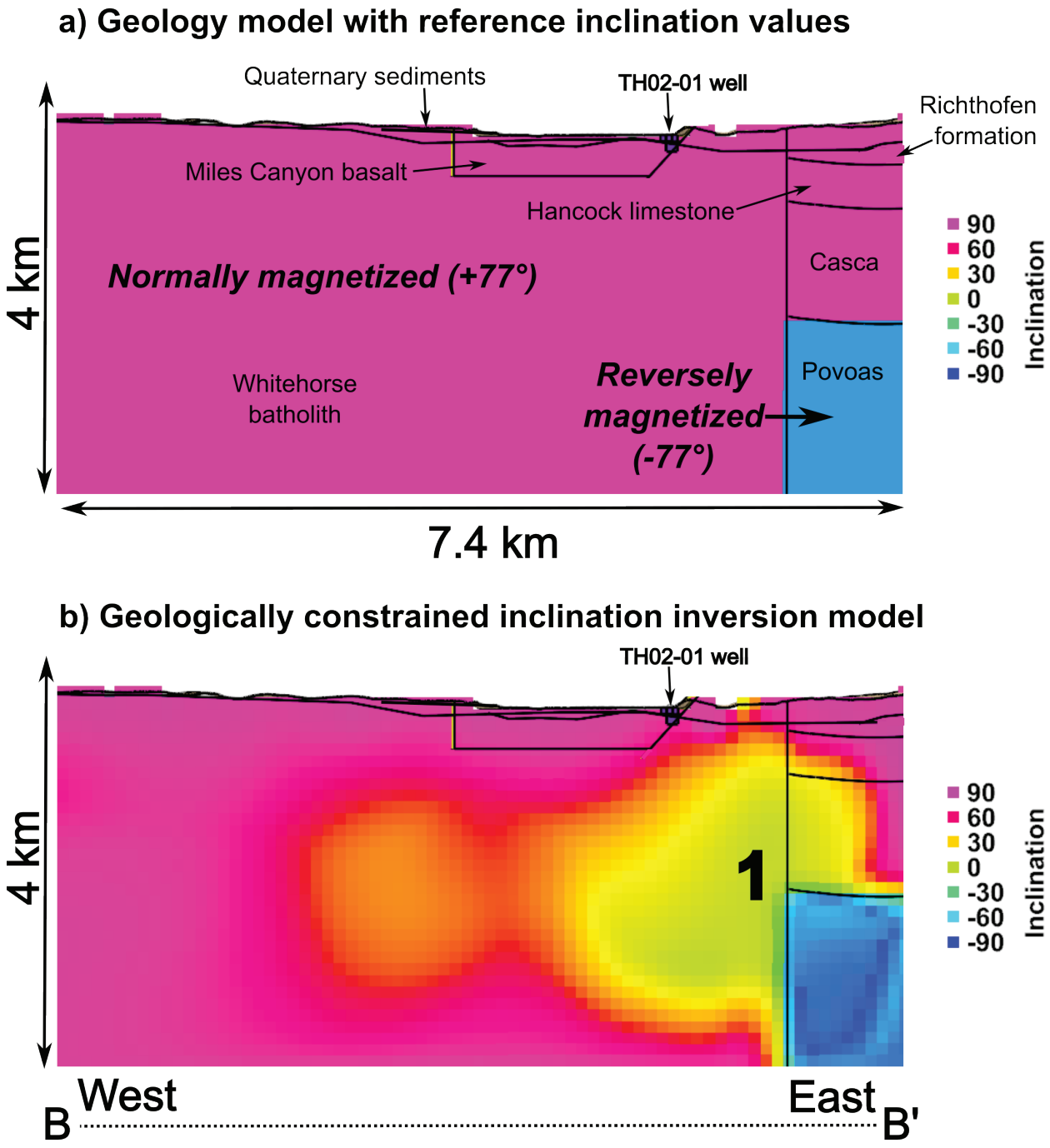

Figure 26. *Inclination model cross-sections along B-B' through the Miles Canyon basalt.* ***a)*** *Geology model with reference inclination values used to constrain the MVI modelling.* ***b)*** *Inclination distribution returned by the 3D MVI inversion modelling that honours the regional-scale magnetic survey data. The match between the reference inclination (a) and the inverted inclination model (b) is fair but it is particularly poor in location 1. See text for further explanation.*

Depth-to-bedrock model

The 3D geologic model generated in this study was used to construct a depth-to-bedrock map for the area covered by the gravity survey (Fig.27). This depth-to-bedrock map estimates the thickness of Quaternary sediments on top of the bedrock. Sediment thicknesses less than 10 m are unable to be discerned because that is the thickness of the smallest cell size used in the modelling. Overall, the greatest thickness of sediment cover lies in the NE quadrant of the study area where the depth to the top of the bedrock reaches ~350 m. In the western half of the study area, the depth-to-bedrock is generally less than 100 m. The uncertainties in the depth-to-bedrock calculations are estimated to be ±40 m in the near surface and up to ±100 m in the deepest parts of the Quaternary sediment pile. This depth-to-bedrock model is comparable to that of Pearson et al. (2001) but contains more detail in the NE quadrant of the study area where well data are lacking.

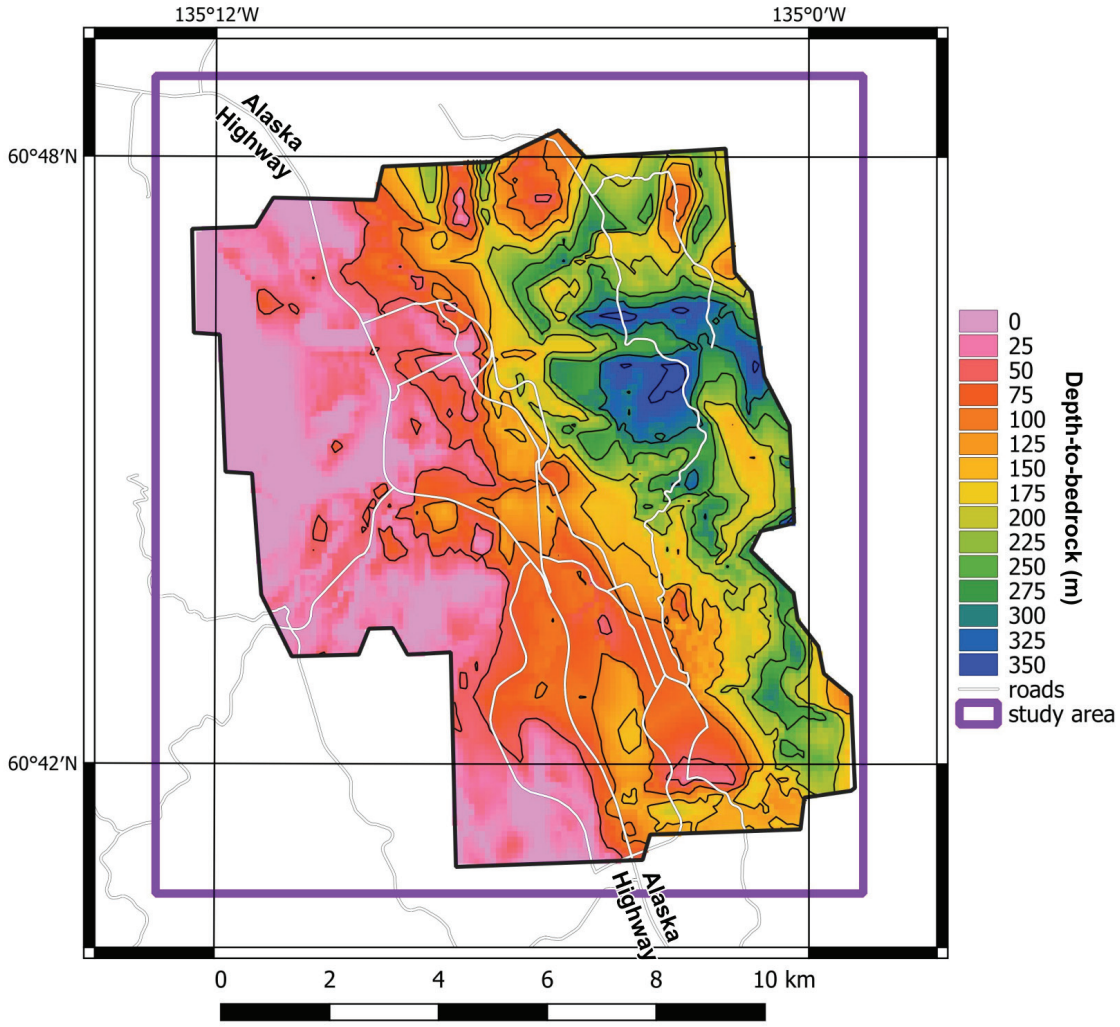

Figure 27. *Depth-to-bedrock map for the Whitehorse area. Contour interval is 50 m. The depth-to-bedrock map covers the portion of the study area with gravity data since gravity data were required for modelling the thickness variation of the glacial sediments.*

Discussion – Implications for geothermal resources

Temperature

Our understanding of subsurface temperature in the Whitehorse area comes from multiple sources. Regional-scale heat flow measurements of ~80 to 100 mW/m^2 (Lewis et al., 2003) suggest elevated subsurface temperatures across southern Yukon which are at odds with the one heat flow measurement of 60 mW/m^2 (also reported by Lewis et al., 2003) obtained from the Whitehorse Copper-3 borehole. This hole yielded a low temperature gradient(~20°C/km) and was apparently drilled into a relatively 'cold' Whitehorse batholith. Elevated subsurface temperatures at a regional-scale are also suggested by CPD mapping which give a crustal-scale temperature gradient of ~42 to 48°C/km for the greater Whitehorse area.

Aside from the Whitehorse Copper-3 borehole, downhole temperature profile measurements in the study area cover a wide range such as ~37°C/km at the TH02-01 well, that was completed in the Miles Canyon basalt aquifer, and 62°C/km in well TH4-76 that was completed at shallow levels (36 m) in glacial sediments. In addition, silica geothermometry calculations from water samples collected at the warm springs yield geothermal reservoir temperature estimates of 54 to 87°C. Furthermore, the geothermal waters that feed the warm springs may be heated by the nearby Haeckel Hill pluton which has radiogenic heat production values above the global average.

Taken together, this information can be used to estimate the range in possible depths of a geothermal reservoir that feeds the warm springs (Table 3). Comparing these depth estimates with the 3D geology model constructed for this study would suggest that a geothermal reservoir located directly beneath the warm springs would reside in either the Casca member of the Aksala formation (at shallower levels) or the Povoas formation (at greater depths).

Table 3. *Possible depths (in km) of the geothermal reservoir beneath the Versluce and Stinky Lake warm springs based upon silica geothermometry estimates and the range in measured temperature gradients from wells in the Whitehorse area.*

Warm spring	Reservoir temp. (°C)	Temperature gradient		
		20 °C/km	37 °C/km	62 °C/km
Versluce	54 °C	2.7 km	1.5 km	0.9 km
Stinky Lake	87 °C	4.4 km	2.4 km	1.4 km

Unfortunately, the subsurface temperature gradient near the warm springs has not been measured and is, therefore, not accurately known. Thus, an accurate prediction of the subsurface temperature and depth to the reservoir is difficult. The drilling of an exploratory borehole would be required to better ascertain the temperature gradient below the warm springs.

The maximum potential temperature of aquifers hosted in glacial sediments can be estimated by combining temperature gradient data from wells with the depth-to-bedrock estimates from this study. Since subsurface temperature increases with depth in the Earth, the hottest sediment-hosted aquifers would be located at the bottom of the thickest stack of Quaternary sediments. For the Whitehorse area, the maximum thickness of glacial sediments is estimated to be ~350 m (Fig. 27). Using the range in temperature gradient values measured in wells (20–62°C/km) yields a sediment-hosted aquifer temperature with the range 7 to 22°C. Thus, a geothermal development program that targets only geothermal aquifers hosted by glacial sediments would likely yield modest temperatures.

Permeability

Rock permeability, the ability of fluid to flow through the rock, is an additional key requirement for a conventional (i.e., not engineered) geothermal system to be viable. Three types of subsurface permeability are discussed here.

Fracture permeability

In many cases, geothermal systems are controlled by complex networks of faults and fractures in rock that allow hot geothermal fluids to ascend to shallow areas. Careful mapping of such geologic structures can help pinpoint the location of the geothermal system in the subsurface (e.g., Faulds and Hinz, 2015). Such an approach is difficult in the Whitehorse area, largely because fault structures in the bedrock are obscured by the glacial sediment cover. Similarly, it is difficult to map the fault structures in the study area using geophysical data because of a lack of strong rock property contrasts between the different rock units.

Three faults occur on the west side of the study area near the margin of the Whitehorse batholith trending E-W to NNE-SSW (Fig. 3). None of these faults show evidence of recent movement. Furthermore, analysis of the available geophysical data did not identify any fault step-overs or other variations along strike of the faults which might indicate a zone of potential permeability.

However, NE-SW oriented fault structures located west of the warm springs are in an orientation that may be permeable because they run parallel to the regional compression direction. In addition to the mapped faults, other NE-SW oriented structures are apparent in the high-resolution magnetic survey data. These favourably oriented structures may be important, fractured pathways that allow ascent of geothermal fluids to the warm springs.

Aside from fractures created by faulting, there may be additional fractures in bedrock generated by folding of brittle rock. Specifically, the NW-trending anticline that folds the sedimentary rocks of the Aksala formation in the NW quadrant of the study area hosts brittle lithologies such as limestone.

Stratigraphic permeability

An alternative to fracture permeability in geothermal systems is stratigraphic permeability. Stratigraphic permeability involves sub-horizontal layers of porous and permeable rock, lying at a certain depth below the surface in which warm geothermal fluids could reside. Good examples of such rock types would be gravel, coarse-grained sandstone and karstic carbonate rocks (e.g., limestone with portions of it dissolved away).

Some parts of the glacial sediment pile in the Whitehorse area consist of impermeable, fine-grained lake sediment (mud and silt) while other portions consist of coarse-grained, permeable sand and gravel. As discussed earlier, the temperature of such glacial sediment hosted aquifers is likely in the range of 7 to 22°C with the hottest temperatures restricted to the bottom of the thickest accumulations of glacial sediments.

Stratigraphic permeability could also potentially be found in the carbonate rich portions of the Hancock and Casca members of the Aksala formation if dissolution of the carbonate has occurred. The amount of karstification and void-space development that has occurred (if any) in the Hancock and Casca rock units is unknown.

Permeability at intrusive contacts

Another area of potential subsurface permeability is the geologic contact between igneous intrusions and country rock. This can happen because igneous intrusions are emplaced at elevated temperatures, and upon cooling, thermal contraction can create permeability along the margins of the igneous intrusion (Gilbert et al., 2018). Two rock units from the study area, the Haeckel Hill pluton and the Whitehorse batholith, are bounded by intrusive contacts that are fairly well demarcated by the high-resolution magnetic survey data.

Many of the geologic contacts for the Whitehorse batholith have an unfavourable orientation perpendicular to the regional compression direction. Structures in this orientation would be more likely pressed shut and impermeable. In contrast, a portion of the contact for the Haeckel Hill pluton (mostly outside the study area) has a favourable orientation parallel to the regional compressional direction (NE-SW). In this orientation, existing fractures are more likely to be permeable. However, this study did not find any corroborating evidence for permeability at these intrusive contacts.

Proposed drilling locations

The most prospective areas for further geothermal exploration in Whitehorse are: the NW quadrant of the study area near the warm springs (Area A in Figure 28); and the region near the Miles Canyon basalt (Area B in Figure 28). The NW quadrant of the study area is prospective because of the following:

- The presence of the warm springs;
- Potential fracture permeability associated with the anticlinal fold;
- Potential fracture permeability related to NE and NNE-trending faults;
- Reports of open water at the surface in winter;
- Proximity to the radiogenic Haeckel Hill pluton;
- Possibility of radiogenic plutonic rocks intruded beneath the warm springs as suggested by 3D geophysical modelling.

For these reasons, specific locations for three exploratory boreholes are proposed, located near the Versluce and Stinky Lake warm springs (Fig. 29). These two springs provide direct evidence of warm geothermal fluids in the subsurface, possibly up to 87°C (based on geothermometry estimates) and, therefore, offer the lowest drilling risk to target the highest temperatures in the Whitehorse area. Exploratory drilling at the Crestview warm springs, located in the NW corner of the study area, is not recommended at this time because of limited data and lack of road access.

The three proposed exploratory boreholes are described here and listed in Table 4.

Site #1 is located ~100 m NE of the Versluce warm spring on a private access road. A 1 km deep borehole is recommended to better constrain the subsurface stratigraphy as well as test subsurface temperature and permeability (Fig. 30). According to the 3D geologic model, this borehole would encounter Mandanna sandstone, Hancock limestone and reach the top of the Casca member of the Aksala formation. This borehole would be particularly useful since it would test the geothermal characteristics of all three of these rock units and would help answer the question: Are the geothermal fluids ascending vertically through the Hancock limestone? Or do they ascend at an angle ‘updip’ along an impermeable contact between the Hancock and Mandanna members?

Site #2 is located ~750 m NE of the Versluce warm spring in the parking lot of the Jack Hulland Elementary School. A 1 km deep borehole is recommended here also (Fig. 30). According to the 3D geologic model, the borehole would pass through Mandanna sandstone and reach the top of the Hancock limestone at the bottom of the hole. A borehole at Site #2 is meant to test whether geothermal fluids are flowing 'updip' along the Hancock-Mandanna contact. If they are, Site #2 would be able to sample those geothermal fluids from a depth of 1 km, much deeper than where the Site #1 borehole meets the Hancock-Mandanna contact (~150 m).

Site #3 is located ~550 m ENE of the Stinky Lake warm spring in a wide gravel area on the west side of Pine Street. Again a 1 km deep borehole is recommended and according to the 3D geologic model, the borehole would pass through about 500 m of Hancock limestone and ~500 m of Casca member rocks (Fig. 31). An exploratory borehole at Site #3 provides the opportunity to test the subsurface temperature and permeability of significant thicknesses of both of these rock units. This location ENE of the Stinky Lake warm spring was selected because it lies approximately along strike with the NE-trending Porter Creek fault and it also is road accessible. An exploratory borehole positioned at the Stinky Lake warm spring is not considered here because of limited road access. A borehole on the west side of Stinky Lake warm spring is not recommended because the Whitehorse Copper #2 well was drilled in

Table 4. *Locations of proposed drill sites in UTM NAD83 Zone 8 coordinates.*

Proposed drill site	UTM easting	UTM northing
#1	492140	6736289
#2	492704	6736588
#3	493549	6735428

1976 at a location about 200 m WSW of the warm spring to a depth of 213 m with a modest temperature gradient of only ~23°C/km.

The Miles Canyon basalt, in the SE corner of the study area (Area B in Figure 28), is also prospective for low temperature geothermal resources. The subsurface in this area has been shown to be permeable and hosts groundwater warmed to modest temperatures (9°C in the bottom of well TH02-01) by the background geothermal gradient. Such low temperature geothermal fluids can be useful for ground-source geothermal heat pump systems. However, to maximize the value of geothermal fluids extracted from the Miles Canyon basalt, the target should be permeable rocks where the fluid temperature is highest. Such a location would be at the base of the thickest portion of the Miles Canyon basalt pile. The base of the Miles Canyon basalt is likely permeable because the bottom portions of lava flows commonly consist of coarse rubble. Furthermore, the bottom of the thickest portion of the lava pile would be located deeper underground and have higher temperatures than the thinner portions of the Miles Canyon basalt. The existing geological, geophysical and water well data is not sufficient to map out the thickness variations of the Miles Canyon basalt to pinpoint where it is the thickest. Therefore, exploratory drilling in the Miles Canyon basalt is not recommended at this time. Geophysical surveys designed to image the Miles Canyon basalt in 3D are needed prior to selecting drill targets in this part of Whitehorse.

The central and SW portions of the study area are not considered geothermally prospective because glacial sediments in this area are relatively thin (<50 m). and they are underlain in many areas by Whitehorse batholith bedrock which is generally characterized by low temperature gradients in the subsurface.

Furthermore, exploratory boreholes in the NE quadrant of study area are not recommended at this time because of: a) limited road access; b) distance from populated areas; and c) limited

thickness of glacial sediments (max. 350 m) restricts sediment-hosted geothermal aquifers to modest temperatures (7–22°C). Beneath the glacial sediments in this part of the study area reside significant thicknesses of sedimentary rocks of the Whitehorse trough. The potential permeability and temperature of geothermal aquifers hosted in Whitehorse trough rocks is relatively unknown due to a lack of deep drilling.

Key questions that may be answered by an exploratory drilling program at the three proposed drilling locations include:

- How thick is the sediment cover at the proposed drill site?
- What is the permeability of the glacial sediments?
- What is the temperature gradient and heat flow?
- What are the thicknesses of the different rock units in the Aksala formation that underlie the warm springs and are they fractured/permeable?
- Do any of the sedimentary rocks of the Aksala formation host geothermal aquifers?
- Are plutonic rocks intruded in the subsurface beneath the drill sites and, if so, what kind?
- If water is encountered in the well, what does the subsurface water chemistry tell us about the temperature of potential geothermal source aquifers (i.e., geothermometry)?

Answers to these questions are important to obtain because they will have significant implications for future development of geothermal resources at Whitehorse.

Direct use geothermal applications that could be pursued based upon the expected fluid temperatures mentioned above include geothermal heat pumps, aquaculture, hot tubs, snow melting and de-icing, greenhousing, building heating, water heating and food drying.

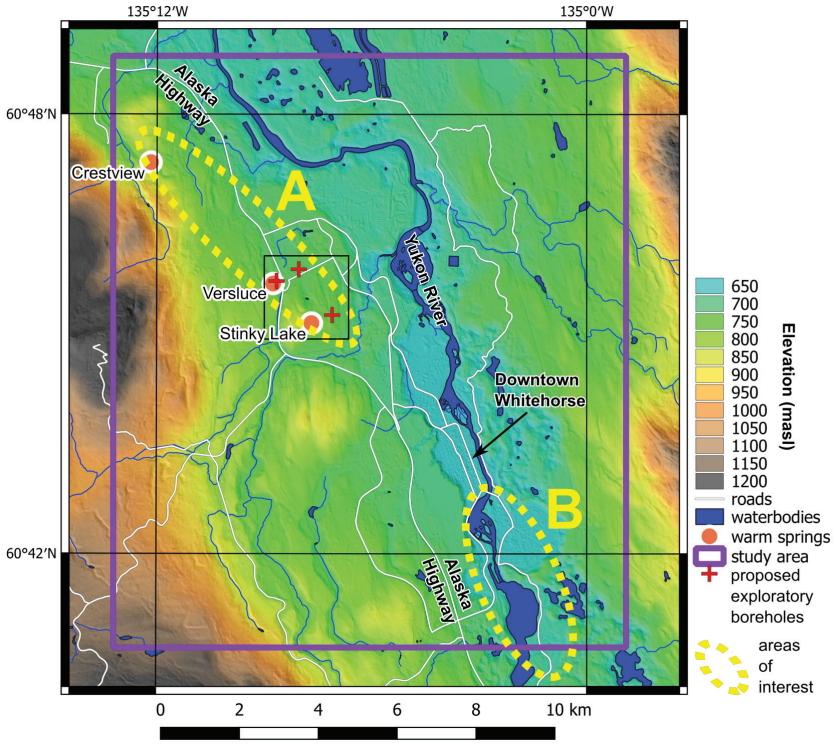

Figure 28. *Overview map of the Whitehorse study area showing two areas of interest (yellow ovals) to focus future geothermal exploration efforts as well as specific locations of three proposed exploratory boreholes (red crosses). See text for discussion. Black box identifies the location of the detail area shown in Figure 29.*

Figure 29. *Satellite image focused on the Versluce and Stinky Lake warm springs area with the locations of the three proposed exploratory boreholes shown. The location of this figure in the context of the entire Whitehorse study area is shown in Figure 28.*

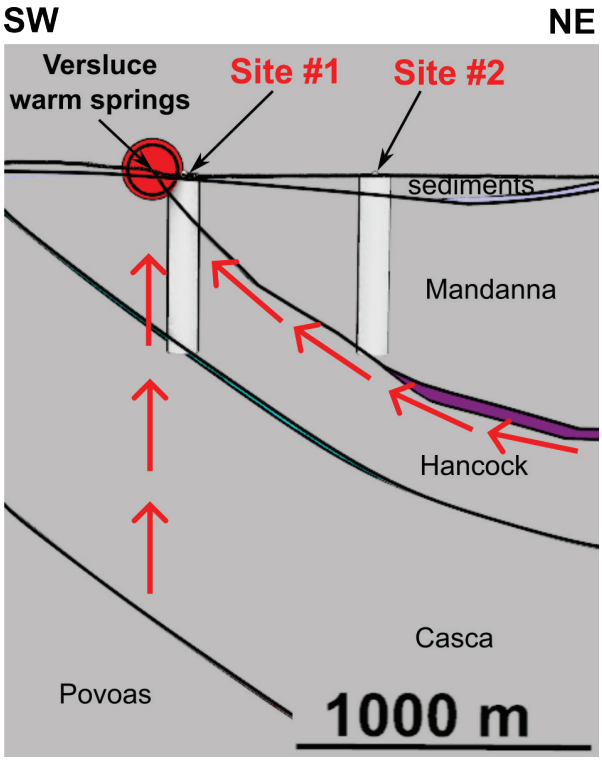

Figure 30. *Geologic cross section showing the locations of the two proposed, 1000 m deep, exploratory boreholes (white) located NE of Versluce warm spring. Red arrows represent two hypotheses of geothermal fluid flow: vertical ascent or inclined ascent along the contact between Mandanna and Hancock units.*

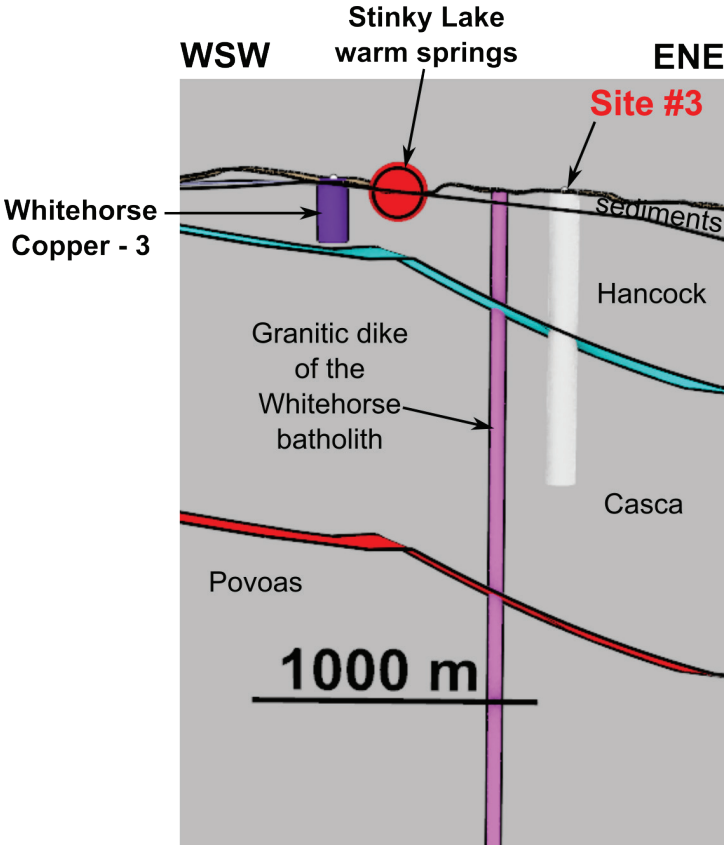

Figure 31. *Geologic cross section showing the location of the proposed, 1000 m deep, exploratory borehole (white) located ENE of Stinky Lake warm springs.*

Conclusions

This study analyzed and interpreted an array of geoscience data within and around the City of Whitehorse in southern Yukon. The primary goal of the study was to better understand the potential for geothermal energy resources in the area with a focus on subsurface temperature and permeability. Interest in the geothermal potential near Whitehorse is due to: a) multiple lines of evidence supporting above average temperature gradient in southern Yukon; b) the presence of warm springs in the Porter Creek and Crestview subdivisions; and c) a desire to use geothermal resources for heating purposes in Whitehorse. Key geoscience datasets interpreted in this study include: bedrock geology maps, surficial geology maps, fault maps, rock properties, radiogenic heat production, gravity, magnetics, lidar topography, warm spring water chemistry and water wells.

Three-dimensional, geologically constrained modelling of gravity and magnetic data was employed to help characterize the 3D geometry of the major rock units in the study area. One outcome of this effort is a depth-to-bedrock map for Whitehorse that characterizes the varying thickness of glacial sediments. The NE quadrant of the study area has the greatest depth-to-bedrock and reaches a depth of ~350 m. The western half of the study area is covered by much thinner accumulations of glacial sediments (i.e., <50 m). Moderate temperature geothermal resources (7–22°C) may be found at the base of the thickest sections of glacial sediments; however, the NE portion of the study area has limited road access. Areas underlain by the granitic rocks of the Whitehorse batholith are considered geothermally unfavourable.

Some of the rock units in the Whitehorse area have similar rock property values (i.e., density and magnetic properties) which make it difficult to distinguish one bedrock unit from another.

But 3D modelling of gravity data suggests that radiogenic granite from the Haeckel Hill pluton may be present beneath the warm springs and may be the heat source for the springs. In addition, the 3D geologic model and warm spring chemistry data both agree that limestone rock units beneath the warm springs may be the host of the geothermal reservoir that feeds the springs. Three specific locations for 1 km deep exploratory boreholes are proposed near the warm springs to collect information on subsurface stratigraphy, temperature and permeability. Low temperature geothermal reservoirs associated with the Miles Canyon basalt rock unit in southeastern Whitehorse also merit further geoscience study to better identify drilling locations.

Recommendations for future work

This geothermal study has been able to leverage large amounts of pre-existing, high quality geoscientific data thanks to years of effort by the Yukon Geological Survey. The drilling of new wells to depths of 1 km in the vicinity of the warm springs would answer many questions about the subsurface. Further geoscience data collection and analysis to help geothermal exploration in the Whitehorse area includes:

1. Collection of audio magnetotelluric (AMT) data in the SE part of the study area to help map the subsurface extent and thickness of the Miles Canyon basalt unit.
2. Collection of MT data in the NW part of the study area to help map the subsurface stratigraphy and, possibly, the subsurface extent of the Haeckel Hill pluton to better understand how it may provide heat to the warm springs.
3. Passive seismic studies would be helpful as an additional technique to estimate the depth-to-bedrock and, potentially, detect microseismic events along faults in the study area.
4. Additional geologic mapping and rock property data collection at outcrops at the eastern end of the Haeckel Hill pluton would help to better refine the understanding of the origins of the elevated gravity and magnetic response in that area.
5. Map the abundance and orientation of natural fractures and jointing in Aksala formation rocks to determine if rock permeability may be elevated due to folding in these rocks.
6. Collect more detailed gravity data (i.e., decreasing the station spacing from 500 to 250 m) in the NW quadrant (vicinity of warm springs) and SE quadrant (vicinity of Miles Canyon basalt) to better characterize the subsurface geology, and at the same time fill the gravity data gap that currently exists at the Whitehorse airport.
7. Use a drone to collect magnetic survey data at high resolution (i.e., 100 m line spacing) immediately east of the warm springs to then merge with the existing high-resolution magnetic data from Gladiator Metals Corp. to better characterize subsurface structure and stratigraphy.
8. Use a drone to collect magnetic survey data at high resolution (i.e., 100 m line spacing) in the SE quadrant of the study area to help map the spatial extent of the Miles Canyon basalt rock unit.
9. Analyse warm springs and water wells for $^{3}He/^{4}He$ ratios to spatially map the areas which are likely fed by a deep crustal component of geothermal fluids.
10. Collect rock samples from the three members of the Aksala formation (Mandanna, Hancock and Casca) and determine the porosity and permeability of these rock units.

Acknowledgments

This project benefited greatly from discussions with Maurice Colpron about bedrock geology and structure of southern Yukon. Craig Hart is also thanked for his helpful comments based upon his extensive experience mapping the geology of the Whitehorse area. Maurice Colpron and Jan Dettmer provided helpful reviews of this report which improved the text. We also thank the Kwanlin Dün First Nation and Ta'an Kwäch'än Council for this opportunity to work on this interesting project on their traditional lands.

References

Aurora Geosciences Ltd. and Bruce, J.O., 2020. Reprocessing of Yukon magnetic data for NTS 105D. Yukon Geological Survey, Open File 2020-12, scale 1:250 000, 4 sheets, https://data.geology.gov.yk.ca/Reference/95845.

Aurora Geosciences Ltd., 2024. Whitehorse area DEM compilation. Unpublished technical report for Yukon Geological Survey, 15 p.

Bond, J.D., Morison, S. and McKenna, K., 2005a. Surficial geology of MacRae (NTS 105D/10), Yukon (1:50 000 scale). Yukon Geological Survey, Geoscience Map 2005-6, https://data.geology.gov.yk.ca/Reference/42767.

Bond, J.D., Morison, S. and McKenna, K., 2005b. Surficial geology of Whitehorse (NTS 105D/11), Yukon (1:50 000 scale). Yukon Geological Survey, Geoscience Map 2005-7, https://data.geology.gov.yk.ca/Reference/42768.

Bond, J.D., Morison, S. and McKenna, K., 2005c. Surficial geology of Upper Laberge (NTS 105D/14), Yukon (1:50 000 scale). Yukon Geological Survey, Geoscience Map 2005-8, https://data.geology.gov.yk.ca/Reference/42769.

Cockett, R., Kang, S., Heagy, L.J., Pidlisecky, A. and Oldenburg, D.W., 2015. SimPEG: An open-source framework for simulation and gradient based parameter estimation in geophysical applications. Computers and Geosciences, vol. 85, p. 142–154, https://doi.org/10.1016/j.cageo.2015.09.015.

Colpron, M., 2019. Potential radiogenic heat production from granitoid plutons in Yukon. Yukon Geological Survey, Open File 2019-16, 1 map and data, https://data.geology.gov.yk.ca/Reference/95816.

EBA Engineering Consultants Ltd., 2008. Groundwater temperature, geothermometer, and geothermal signature assessment, City of Whitehorse, Yukon. Technical report prepared for City of Whitehorse, Dated July 24, 2008, 56 p.

EBA Engineering Consultants Ltd., 2009. Hydrogeochemistry and isotope signature of Stinky Lake and Versluce warm springs in Whitehorse, Yukon – W23101159.014. Technical report prepared for Yukon Energy Corporation, Dated October 30, 2009, 28 p., https://data.geology.gov.yk.ca/Reference/95995.

EBA Engineering Consultants Ltd., 2010a. Summary report 2009 geothermal exploration program, multiple areas, Yukon – W23101159.031. Consultant report for Yukon Energy Corporation, April 2010, 35 p., https://data.geology.gov.yk.ca/Reference/96008.

EBA Engineering Consultants Ltd., 2010b. Noble gas data from multiple warm and hot springs in southern and central Yukon – W23101159.022. Technical report prepared for Yukon Energy Corporation, Dated March 31, 2010, 18 p., https://data.geology.gov.yk.ca/Reference/96003.

EBA, A Tetra Tech Company, 2011a. Geology and hydrogeochemistry of the Stinky Lake warm spring, Whitehorse, Yukon – W23101159.105. Technical report prepared for Yukon Energy Corporation, Dated March 31, 2011, 30 p., https://data.geology.gov.yk.ca/Reference/96014.

EBA, A Tetra Tech Company, 2011b. Geophysical survey at Stinky Lake, Whitehorse – W23101159.106. Technical report prepared for Yukon Energy Corporation, Dated April 2011, 17 p., https://data.geology.gov.yk.ca/Reference/96015.

EBA, A Tetra Tech Company, 2012. Preliminary geothermal assessment Vista Mountain warm springs north of Whitehorse, Yukon – W23101579.004. Technical report for Yukon Energy Corp., 53 p., https://data.geology.gov.yk.ca/Reference/96018.

Faulds, J.F. and Hinz, N.H., 2015. Favorable tectonic and structural settings of geothermal systems in the Great Basin region, western USA: Proxies for discovering blind geothermal

systems. Proceedings World Geothermal Congress 2015, Melbourne, Australia, 19–25 April 2015, 6 p.

Fournier, D. and Oldenburg, D., 2019. Inversion using spatially variable mixed Lp norms. Geophysical Journal International, vol. 218, no. 1, July 2019, p. 268–282, https://doi.org/10.1093/gji/ggz156.

Fournier, D., Heagy L.J. and Oldenburg, D.W., 2020. Sparse magnetic vector inversion in spherical coordinates. Geophysics, vol. 85, no. 3, p. J22-J49, https://doi.org/10.1190/geo2019-0244.1.

Fullagar, P.K. and Pears, G.A., 2007. Towards geologically realistic inversion. In: Proceedings of Exploration 07: Fifth Decennial International Conference on Mineral Exploration, B. Milkereit (ed.), Toronto. p. 444–460.

Fullagar, P.K., Pears, G.A. and McMonnies, B., 2008. Constrained inversion of geologic surfaces—Pushing the boundaries. The Leading Edge, vol. 27, p. 98–105, https://doi.org/10.1190/1.2831686.

Fraser, T.A., Grasby, S.E., Witter, J.B., Colpron, M. and Relf, C., 2018. Geothermal studies in Yukon – Collaborative efforts to understand ground temperature in the Canadian North. GRC Transactions, vol. 42, 20 p.

Gartner Lee Limited, 2003. Vanier School ground source heat pump project – Hydrogeological assessment. Technical report prepared for Energy Solution Center Inc., reference# GLL 22-292, 49 p.

Gaudreau, É., Audet, P. and Schneider, D. A., 2019. Mapping Curie depth across western Canada from a wavelet analysis of magnetic anomaly data. Journal of Geophysical Research: Solid Earth, vol. 124, p. 4365–4385, https://doi.org/10.1029/2018JB016726.

Gilbert, L.A., Crispini, L., Tartarotti, P. and Bona, M.L., 2018. Permeability structure of the lava-dike transition of 15 Myr old oceanic crust formed at the East Pacific Rise. Geochemistry, Geophysics, Geosystems, vol. 19, p. 3555-3569, https://doi.org/10.1029/2018GC007696.

Government of Yukon, 2018. Yukon's energy context. Energy Branch, Department of Energy, Mines, and Resources, 12 p., https://yukon.ca/sites/yukon.ca/files/emr/emr-yukon-energy-context.pdf.

Hart, C.J.R., 1997a. Geology of Upper Laberge map area, southern Yukon, (NTS 105 D/14). Exploration and Geological Services Division, Yukon, Indian and northern Affairs Canada, Geoscience Map 1997-5, 1:50 000 scale, https://data.geology.gov.yk.ca/Reference/42403.

Hart, C.J.R., 1997b. A transect across Stikinia: Geology of the northern Whitehorse map area, southern Yukon Territory (105D/13-16). Exploration and Geological Services Division, Yukon, Indian and northern Affairs Canada, Bulletin 8, 112 p., https://data.geology.gov.yk.ca/Reference/42215.

Hart, C.J.R. and Radloff, J.K., 1990. Geology of Whitehorse, Alligator Lake, Fenwick Creek, Carcross and part of Robinson map areas (105D/11, 6, 3, 2, & 7). Exploration and Geological Services Division, Yukon, Indian and northern Affairs Canada, Open File 1990-4, 126 p., https://data.geology.gov.yk.ca/Reference/42405.

Hart, C.J.R. and Villeneuve, M., 1999. Geochronology of Neogene alkaline volcanic rocks (Miles Canyon basalt), southern Yukon Territory, Canada: the relative effectiveness of laser 40Ar/39Ar and K–Ar geochronology. Canadian Journal of Earth Sciences, vol. 36, no. 9, p. 1495-1507, https://doi.org/10.1139/e99-049.

Hasterok, D. and Webb, J., 2017. On the radiogenic heat production of igneous rocks. Geoscience Frontiers, vol. 8, no. 5, p. 919-940, https://doi.org/10.1016/j.gsf.2017.03.006.

Hyndman, R.D., Cassidy, J.F., Adams, J., Rogers, G.C. and Mazzotti, S., 2005. Earthquakes and

seismic hazard in the Yukon-Beaufort-Mackenzie. Recorder, vol. 30, no. 5, 16 p.

Langevin, H., Fraser, TA. and Raymond, J., 2020. Assessment of thermo-hydraulic properties of rock samples near Takhini Hot Springs and in the Tintina fault zone, Yukon. Yukon Geological Survey, Miscellaneous Report 19, 30 p., https://data.geology.gov.yk.ca/Reference/95840.

Léveillée-Dallaire, X. and Raymond, J., 2024. Hydrothermal modelling of Takhini Hot Springs (NTS 105D/14). In: Yukon Exploration and Geology Technical Papers 2023, L.H. Weston and Purple Rock Inc. (eds.), Yukon Geological Survey, p. 77–96, https://data.geology.gov.yk.ca/Reference/96039.

Lewis, T.J., Hyndman, R.D. and Flück, P., 2003. Heat flow, heat generation, and crustal temperatures in the northern Canadian Cordillera: Thermal control of tectonics. Journal of Geophysical Research, vol. 108, no. B6, 2316, https://doi.org/10.1029/2002JB002090.

Li, C.-F., Lu, Y. and Wang, J., 2017. A global reference model of Curie-point depths based on EMAG2. Nature, Scientific Reports, vol. 7, 9 p., https://doi.org/10.1038/srep45129.

Lipovsky, P.S., 2023. Surficial geology and geohazards of the greater Whitehorse area. Yukon Geological Survey, Open File 2023-1, 67 p. plus appendices, https://data.geology.gov.yk.ca/Reference/95981 .

Ogg, J.G., 2012. Chapter 25 – Triassic. In: The Geologic Time Scale 2012, F.M. Gradstein, J.G. Ogg, M. Schmitz and G. Ogg (eds.), Elsevier, p. 681-730, https://doi.org/10.1016/B978-0-444-59425-9.00025-1.

Pearson, F.K., Hart, C.J.R. and Power, M., 2001. Distribution of Miles Canyon basalt in the Whitehorse area and implications for groundwater resources. In: Yukon Exploration and Geology 2000, D.S. Emond and L.H. Weston (eds.), Exploration and Geological Services Division, Yukon, Indian and Northern Affairs Canada, p. 235-245, https://data.geology.gov.yk.ca/Reference/42474.

Siler, D.L. and Kennedy, B.M., 2016. Regional crustal-scale structures as conduits for deep geothermal upflow. Geothermics, vol. 59, p. 27-37, https://doi.org/10.1016/j.geothermics.2015.10.007.

Wheeler, J.O., 1961. Whitehorse Map Area, Yukon Territory 105D. Geological Survey of Canada, Memoir 312, 183 p.

Witter, J.B., Miller, C.A., Friend, M. and Colpron, M., 2018. Curie point depths and heat production in Yukon, Canada. In: Proceedings 43rd Workshop on Geothermal Reservoir Engineering, Stanford University, California, February 12-14, 2018, 11 p.

Witter, J.B., 2024. Analysis of geoscience data for geothermal exploration in the Dakwäkäda (Haines Junction) area, Yukon. Yukon Geological Survey, Open File 2024-3, 44 p. plus appendices, https://data.geology.gov.yk.ca/Reference/96052.

Yukon Geological Survey, 2023a. A digital atlas of terranes for the northern Cordillera. Yukon Geological Survey, http://data.geology.gov.yk.ca/Compilation/2 [Accessed: January 1, 2025].

Yukon Geological Survey, 2023b. Yukon digital bedrock geology. Yukon Geological Survey, http://data.geology.gov.yk.ca/Compilation/3 [Accessed: January 1, 2025].

Yukon Geological Survey, 2024. Geothermal dataset. Yukon Geological Survey, https://data.geology.gov.yk.ca/Compilation/42 [accessed January 1, 2025].

Appendices

Appendix A: Whitehorse gravity data and report; Aurora Geosciences

This appendix is only available digitally. The files are included in a .zip file that accompanies this report, and are available from https://data.geology.gov.yk.ca.

Appendix B: Additional geoscience data files

This appendix is only available digitally. The files are included in a .zip file that accompanies this report, and are available from https://data.geology.gov.yk.ca.

All .shp, .dxf, and .tif files, as well as 3D block models in .txt file format are georeferenced to UTM NAD83 Zone 8 (EPSG: 26908).

Appendix C: Statement of Qualifications

This report has been prepared by Jeffrey B. Witter, Principal Geoscientist at Innovate Geothermal Ltd. Dr. Witter holds an undergraduate degree in geophysics as well as Master's and Ph.D. degrees in geology. He has nineteen years of experience as an exploration geologist/geophysicist in the natural resource industry with more than half of that time committed specifically to geothermal exploration and resource evaluation. He is a registered professional geoscientist in the province of British Columbia (Canada) and is a member of Engineers and Geoscientists of British Columbia (EGBC). EGBC has a defined and enforceable Code of Ethics which Dr. Witter agrees to abide by. Dr. Witter has been engaged as a Consultant by the Yukon Geological Survey but holds no financial interest in any geothermal energy project in the Yukon.

Dated in Vancouver, British Columbia, Canada this _5th_ day of May 2025

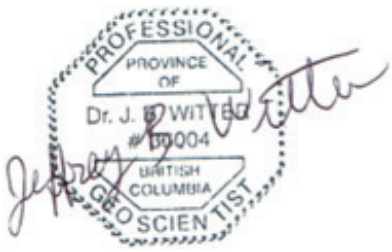

Jeffrey B. Witter Ph.D., PGeo (Province of British Columbia, No. 36004)

Yukon Geological Survey
Energy, Mines and Resources
Government of Yukon